



Multi-site hydrometeorological simulation of streamflow for upper Jhelum basin in northwest Himalayas using HEC–HMS soil moisture accounting algorithm

Taroob Bashir Naqash¹ · Manzoor Ahmad Ahanger¹ · Rajib Maity²

Received: 2 July 2022 / Accepted: 20 August 2022 / Published online: 30 August 2022
© The Author(s), under exclusive licence to Springer Nature Switzerland AG 2022

Abstract

Hydrometeorological influence on run-off is a process-driven mechanism in basin hydrology that needs to be captured for a reliable assessment of the basin-scale hydrological responses in the context of climate change. In this study, one of such process-based model, the Hydrologic Engineering Center–Hydrologic Modeling System model is used to simulate multi-site streamflow in the upper Jhelum basin, northwest Himalayas, India. The soil moisture accounting algorithm was used to calibrate and validate the model for continuous simulation on a monthly timescale at three gauging stations Ram Munshi Bhag, Sangam, and Rambiar. The model was calibrated for a period of 12 years (2003–2014) and validated for 5 years (2015–2019). Observed and simulated streamflow values during the calibration period were found to be in good agreement with R^2 ranging from 0.783 to 0.808, NSE from 0.753 to 0.793, and P.B from 2.7 to 5.1%. Similar performance was obtained during the validation period also with R^2 ranging from 0.80 to 0.83, NSE from 0.70 to 0.80, and PB from 2 to 6.8%. The sensitivity analysis of the model was performed using one-at-a-time analysis method. This helps to rank the parameter according to their sensitivities towards the model performance in simulating run-off volume. Soil storage, soil tension storage, and soil percolation were found to be the most sensitive parameters while groundwater-2 coefficient storage, and percolation were the least sensitive parameters in the basin. The overall model performance was reasonably good, and can be further used for rainfall–run-off simulation in the upper Jhelum basin for the climate change impact related studies in future.

Keywords Calibration · Continuous modeling · HEC–HMS model · Sensitivity analysis · SMA · Validation

Introduction

The variability in climate has greatly impacted the hydrological activities occurring in a watershed. The hydrological models are used to assess these hydrological processes which affect the surface and groundwater flow regimes. The models help in strategizing the sustainability and effective management of the water resources. The insufficient spatial and temporal distribution of data in a watershed leads to the utilization of the hydrological models extensively to

simulate run-off (Kumarasamy and Belmont 2018; Fanta and Sime 2022). Some open-source and popular hydrological modeling software that simulates hydrological components accurately in a watershed include the Soil and Water Assessment Tool (SWAT) (Arnold et al. 1998), the Precipitation Run-off Modelling System (PRMS) (Leavesley et al. 1983; Markstrom et al. 2015), the Systeme hydrologique Europeen (MIKE-SHE) (Graham and Butts 2005), the Variable Infiltration Capacity model (VIC) (Hamman et al. 2018), and the Hydrologic Modelling System (HEC–HMS) (US Army Corps 1998).

The hydrological model selected for any watershed is based on the area of the watershed, data accessibility and accuracy, goal and previous trend of the project, and the efficient and precise utilization of the model (Beven 2011; Sime et al. 2020; Fanta and Sime 2022). In data-scarce regions, it is advisable to use a physically based semi-distributed hydrological model like HEC–HMS (Ramly and Tahir 2016). Semi-distributed models divide the entire

✉ Taroob Bashir Naqash
taroobnaqash@nitsri.net

¹ Department of Civil Engineering, National Institute of Technology Srinagar, Srinagar, Jammu and Kashmir 190006, India

² Department of Civil Engineering, Indian Institute of Technology Kharagpur, Kharagpur, West Bengal 721302, India

basin into several sub-basins called hydrological response units (HRUs) and govern both surface and sub-surface runoff generation processes (Gebre and Ludwig 2015). These models allow the input parameters to partially vary in space to prevent the overparameterization of specific factors that influence the hydrological processes in the basin (Golmohammadi et al. 2014; Kasa et al. 2017).

The Hydrologic Modeling System (HEC–HMS) was perceived as a computer-based problem-solving tool created under the Research and Development Program of US Army Corps of Engineering (USACE). It was first released by the Hydrologic Engineering Center (HEC) in 1992 for simulating the hydrological processes occurring in the basin. The Flood Hydrograph Package HEC-1 and its different specific variants were replaced and substituted by the HEC–HMS hydrological model (US Army Corps of Engineers 2000) and it was named as HEC–HMS version 1.0 and incorporated all the model functionalities of HEC-1 with some improvements. This first generation of the HEC–HMS model focused on simulating individual storm events. The second generation (version 2.0) of the model added new components for infiltration modeling and the soil moisture accounting (SMA) method to allow continuous simulation along with event-based modeling. The third generation (version 3.0) of the model incorporated a new graphical interface and some new methods in the basin model for representing infiltration. Potential evapotranspiration, snowmelt, and reservoir component were added to the third generation HEC–HMS model (Scharffenberg et al. 2010). The fourth significant and innovative arrival of the program was version 4.0 in which surface erosion features and sediment transport were computed. The version 4.0 HEC–HMS added new components to precipitation–run-off–routing simulation, i.e., precipitation–specification options, loss models for computing run-off volume, transform model for transforming excess rainfall, hydraulic routing models for accounting storage, and energy flux, the model for baseflow computation and water control measures (including storage and divergence) (Sahu et al. 2020). This version of model has been used in various studies for achieving goals in reservoir and system operation, flood damage reduction, environmental restoration, water supply planning and management, floodplain regulation, and others.

The HEC–HMS modeling software releases from both present and past utilize simulation components built from conceptual models. These types of hydrological models mostly rely upon empirical data to make predictions about the movement of water. The availability of the calibration data leads to the efficient working of the model. In ungauged watersheds, these types of hydrological models are used effectively.

The efficient working and reliability of the HEC–HMS model are affected by the size and characteristics of the

basin under study (Kabiri et al. 2013). The simulation of rainfall–run-off processes in dendritic type drainage catchments is efficiently represented by the HEC–HMS hydrological model (US Army Corps of Engineers 2000). The hydrological model is built for the basin, by dividing the hydrological cycle into various manageable components and forming boundaries across the basin of interest (US Army Corps of Engineers 2020; Othman et al. 2021). The HEC–HMS model comprises four main components for modeling any watershed: (1) Basin component, (2) Meteorological component, (3) Control specification, and (4) Input data component. For simulating a hydrological model, the calibration and validation processes, and performance evaluation in terms of statistical metrics and sensitivity analysis are very critical issues that need to be considered. One part of the input data is used to calibrate the model satisfactorily and the other part of the data is used to assess the performance of the process of simulation to carry out the validation procedure (Biondi et al. 2012; Ouedraogo et al. 2018). The sensitivity analysis is performed to investigate the most influential parameter in the basin to analyze the impact of each model input parameter on the output. A slight change in the sensitive input parameter can bring enormous changes in the model outcome. The calibration process in hydrological models is an interactive process to improve and evaluate the model input parameters and plays an important role in decreasing ambiguity arising due to the predictions made by the model (Othman et al. 2021). The HEC–HMS hydrological model has been used by several researchers to study the run-off simulation in a basin (Halwatura and Najim 2013; Al-Mukhtar and Al-Yaseen 2019).

Razmkhah et al. (2016) used the HEC–HMS model with the SMA algorithm to model daily streamflow in the Karoon III basin in Iran. The model showed satisfactory performance by evaluating the statistical coefficient, NSE for both calibration and validation periods. The sensitivity analysis of the model showed Clark storage coefficient, saturated hydraulic conductivity, and time of concentration to be the most sensitive parameters in the basin. Bhuiyan et al. (2017) applied the HEC–HMS model in a cold region catchment area and used RADARSAT-2 soil moisture for initializing the model. The satellite data were found to be beneficial for capturing flow peaks generated due to snowmelt events and soil moisture was the most sensitive parameter in the basin. Ouedraogo et al. (2018) used the HEC–HMS SMA model for continuously modeling the streamflow in the Mkurumudzi river watershed in Kenya. The model performed satisfactorily for both calibrations as well as validation periods and soil moisture was found to be the most influential parameter in the study area. Belayneh et al. (2020) evaluated the data acquired from high satellite precipitation products in Dabus catchment, Abbay basin, Ethiopia using the HEC–HMS model to simulate streamflow on daily temporal

and high spatial resolution. The model efficiently predicted watershed run-off for both the satellite rainfall products and the performance of the model improved significantly with the bias-corrected satellite data. Azizi et al. (2021) used the HEC–HMS model to simulate the flood hydrograph under the effect of land-use change in the Ekbatan dam, Iran. After successful calibration and validation of the model, the simulated results indicated an increase in peak discharge volume which in turn increased run-off height. Herath and Wijesekera (2021) developed the HEC–HMS model for evaluating the water resource management in the Maya Oya basin in Sri Lanka. The developed model performed efficiently for both the calibration and the validation periods. Ndeketeya and Dundu (2021) applied the HEC–HMS model to evaluate the rainwater harvesting potential and studied the effect of climate change and seasonal precipitation and socio-economic barriers on rainwater harvesting in Johannesburg semi-arid city. The simulation results revealed that wet season received high volumes of run-off, indicating that rainwater harvesting systems are very feasible and independent of the precipitation seasonality. Mobarhan and Sangchini (2021) applied HEC–HMS SMA for simulating run-off at different calibration scales (monthly, seasonal, semi-annual, annual) in the Zolachay watershed, Iran. The simulation results of the model showed good agreement between the observed and predicted run-off values. The optimized input parameters used for quantifying the annual run-off volume for the monthly calibration period showed more satisfying results than the other time scales.

Ranjan et al. (2022) investigated the basin characteristics and evaluated sub-basin level flood vulnerability using the HEC–HMS model integrated with remote sensing and geographical information system in the Jhelum river. The calibrated and validated hydrological model showed good results when compared with the actual values and sub-basins located on the upstream part of the Jhelum basin were found to be more prone to vulnerability compared to the downstream area. Dimri et al. (2022) used the HEC–HMS model to describe the simulation of streamflow in the Bhagirathi River basin. The model was calibrated and validated from 2010 to 2015 and model simulation results revealed that there exists a good agreement between the observed and the simulated discharge values. Shakarneh et al. (2022) aimed to simulate the rainfall–run-off events in two catchments (Daraja and Al-Ghar) of Palestine using the HEC–HMS model during the 1990–2010 data period. The simulation indicated acceptable model efficiency and suggested that the calibrated HEC–HMS model can be used for forecasting the discharge on small time steps using the rainfall–run-off future climatic scenario. Ben Khélifa and Mosbahi (2022) used the HEC–HMS model to estimate the flood peak discharges and reproduce hydrographs in a small urban ungauged watershed located in North-East of Tunisia. The

results obtained were used to recognize the magnitude of the extreme rainfall events and design the appropriate stormwater structures in urban areas.

The objective of the study is to calibrate and validate the HEC–HMS hydrological model using the SMA algorithm to simulate multi-site monthly run-off in the upper Jhelum basin of the northwest Himalayas using hydrometeorological inputs. Various hydrological processes, such as canopy interception, infiltration, surface depression storage, percolation, soil moisture storage, and groundwater storage were taken into consideration in the SMA algorithm to simulate the continuous relationship between run-off and rainfall, soil losses, and evapotranspiration in the upper Jhelum basin. One-at-a-time (OAT) sensitivity analysis is also carried out to determine the most sensitive parameter in the basin affecting SMA modeling to reduce the uncertainty in the modeling output. The performance of the model was judged by comparing the statistical co-coefficients for simulated and observed discharge values.

Study area

The upper Jhelum basin is spatially located between 33° 22' 4" N–34° 15' 40" N latitude and 74° 30' 35" E–75° 32' 46" E longitude. The elevation of basin ranges between 1567 and 5283 m above mean sea level. The upper Jhelum basin has the Zanskar mountain range on the northeast side and the Pir Panjal range on the southwest side. The origin of the Jhelum river is from the Verinag spring and drains throughout the area. It is one of the major and important tributaries of the Indus river. The upper Jhelum basin constitutes various sub-basins namely Kuthar, Bringi, Vishav, Sandran, Rambiar, Arpal, Romshi, and Liddar and these sub-basins drain their water into the Jhelum river at different locations. The present study area, consisted of four meteorological stations (Pahalgam, Kokernag, Qazigund, and Ram Bagh), and the discharge was estimated at three gauging stations (Ram Munshi Bagh, Sangam, and Rambiar) (Fig. 1).

Datasets for HEC–HMS model

Digital elevation model

The digital elevation model (DEM) having a resolution of 30 m was used for the watershed delineation and estimation of various other watershed characteristics that determine the drainage pattern of the basin. In the current study, SRTM (Shuttle Radar Topography Mission) DEM was downloaded from the USGS (United States Geological Survey) earth explorer (<https://earthexplorer.usgs.gov/>). The slope map for the study area was extracted from the DEM dataset, the

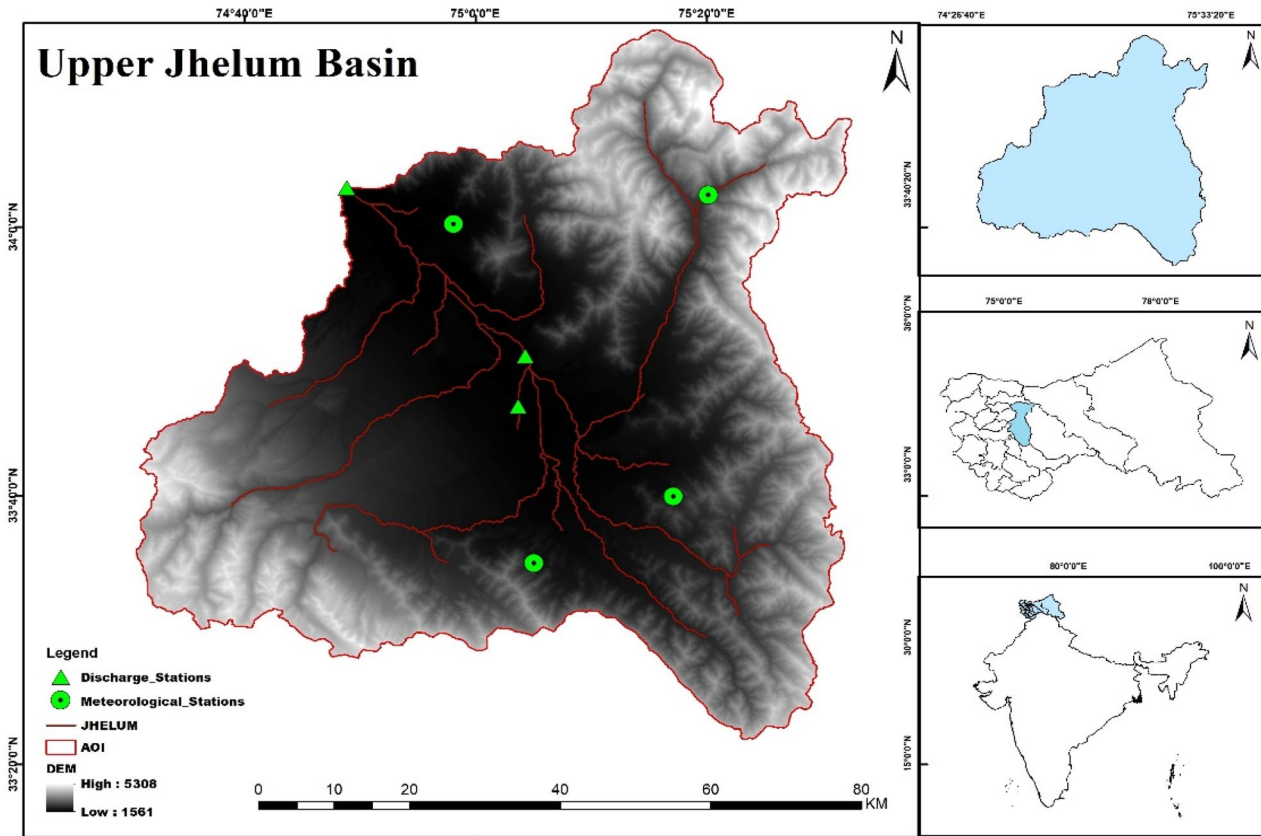


Fig. 1 Geographical location of upper Jhelum basin with spatial distribution of meteorological and streamflow gauging stations

values of which suggest that the study area has a steep slope and a rugged terrain. The DEM and the slope map of the study area are shown in Figs. 2 and 3, respectively.

Land use/cover dataset

The land use/cover dataset is an important factor that affects the hydrological processes like evapotranspiration, run-off, and soil erosion in a basin (Bashir et al. 2018). For the study area, the land use/cover was generated using LANDSAT8 OLI satellite imagery (<https://earthexplorer.usgs.gov/>). The imagery was used in the ERDAS IMAGINE 2014 software for creating different land use classes through a supervised classification algorithm based on National Land Cover Database (NLCD) classification (Fig. 4). The land use consisted of major classes: cultivated crops, developed-medium intensity, evergreen forest, grassland/herbaceous, open water, perennial ice/snow, and shrub/scrub. The land use/cover description is elaborated in Table 1.

Soil dataset

The soil dataset is very important for generating the soil moisture accounting parameters for the HEC–HMS model

and the detailed soil map was obtained from the FAO soil survey of India (<https://www.fao.org>). The soil properties such as texture, saturated hydraulic conductivity, moisture content of the soil, maximum infiltration capacity, maximum tension storage, soil storage, percolation rate, and groundwater percolation rate all depend on the type of soil present in the study area were all derived from the soil data (Fig. 5). There were a total of eleven soil classes present in the study area and their description is given in Table 2.

Evapotranspiration data

Evapotranspiration (ET) plays a critical role when performing continuous modeling. In this study, ET was computed on monthly basis using Thornwaite’s method for the entire basin (Alkaeed et al. 2006; Singh and Jain 2015; Bashir and Kumar 2017). The following Eqs. (1–4) were used to estimate the monthly ET values:

$$ET = 1.6 \left(\frac{10t}{T} \right)^a \left(\frac{n}{12} \right), \quad (1)$$

Fig. 2 DEM of upper Jhelum basin

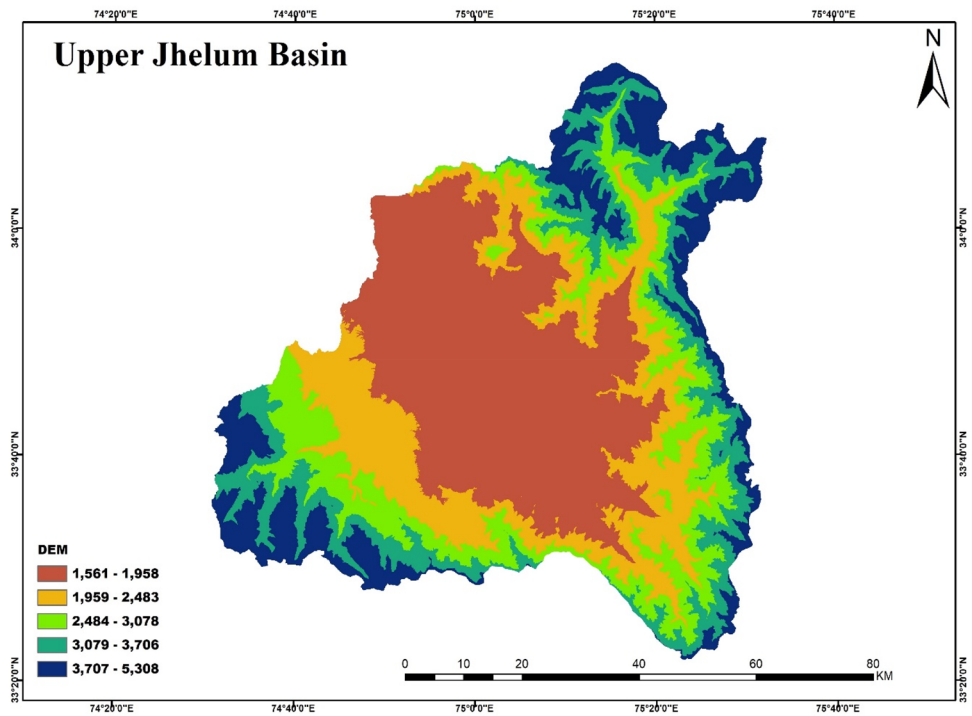
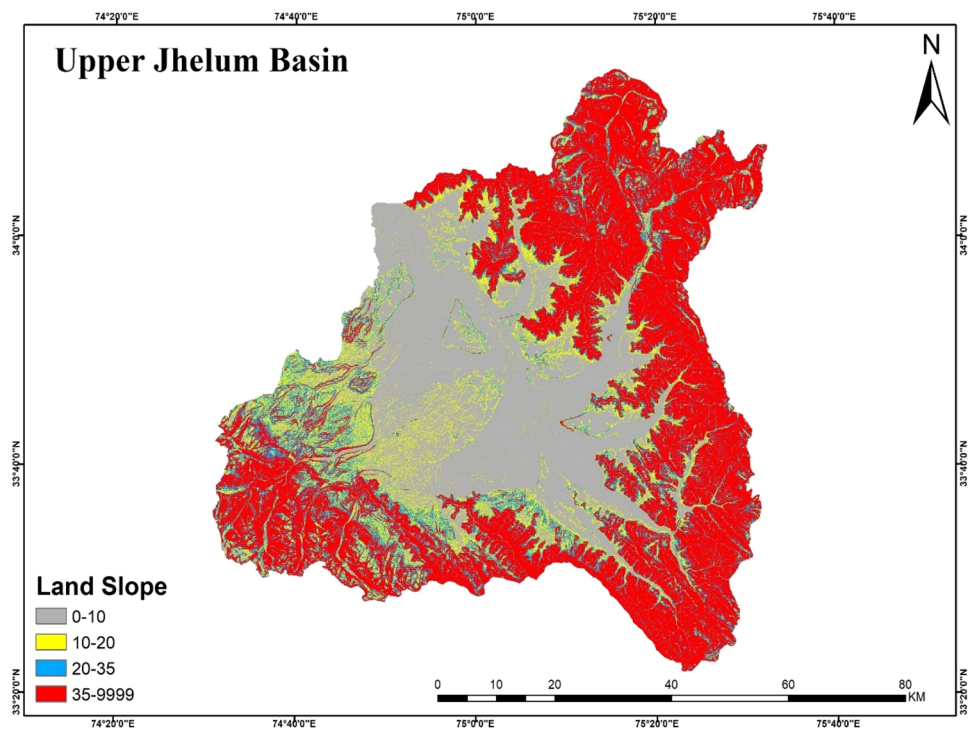


Fig. 3 Slope map of upper Jhelum basin



$$a = 0.000000675(T)^3 - 0.0000771(T)^2 + 0.1792T + 0.49239, \quad (2)$$

$$T = \sum_{i=1}^{12} \left(\frac{t_i}{5}\right)^{1.514}, \quad (3)$$

$$n = 2 \cos^{-1} (-\tan \varphi \tan \delta) \left(\frac{12}{\pi}\right), \quad (4)$$

where ET represents the potential evapotranspiration (cm), T represents Thornwaite's temperature efficiency index,

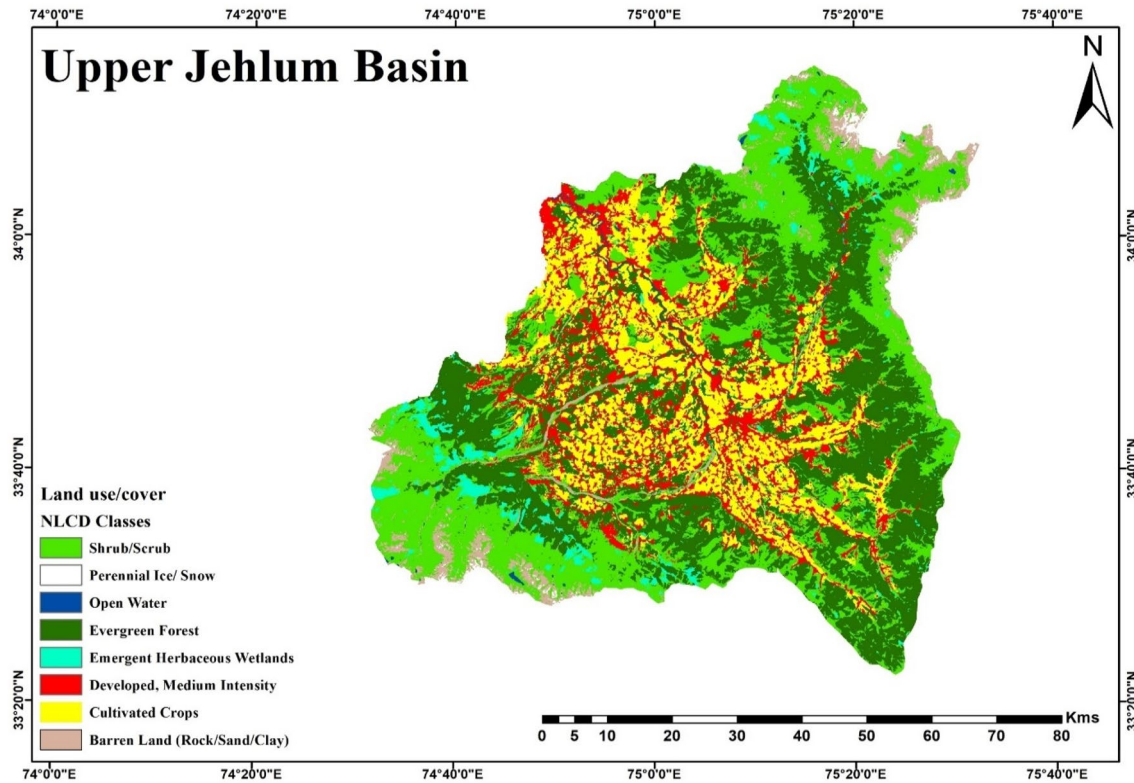


Fig. 4 Spatial variation of land use/cover classes in upper Jhelum basin

Table 1 Description of land use/land cover of upper Jhelum basin

S. no.	NLCD class	Area (km ²)	% Area
1	Shrub/scrub	227.85	4.20
2	Perennial ice/snow	300.10	5.55
3	Open water	566.71	10.46
4	Evergreen forest	1160.01	21.41
5	Emergent herbaceous wetlands	634.56	11.71
6	Developed-medium intensity	195.45	3.61
7	Cultivated crops	1946.28	35.93
8	Barren land (rock/sand/clay)	386.10	7.13
	Total	5417.06	100

n represents average day length of the month, t represents mean monthly air temperature (°C).

Weather data and discharge data

The weather data input in the HEC–HMS model consisted of daily precipitation, daily maximum and minimum temperature, and monthly ET data for four selected weather stations. The daily precipitation, minimum, and maximum temperature data at $0.25^\circ \times 0.25^\circ$ spatial resolution were procured from Indian Meteorological Centre (IMC) Ram Bagh (<https://www.mausam.imd.gov.in>) from 2000 to 2019.

The daily gauge and discharge data were acquired from the Department of Irrigation and Flood control, Kashmir from 2000 to 2019 for three selected discharge stations: Ram Munshi Bagh, Sangam, and Rambiarra (<https://www.ifcka.shmir.com>).

Methodology

HEC–GeoHMS model input

The HEC–GeoHMS is an ArcGIS interface built to process and analyze the geospatial datasets to create input files for the HEC–HMS model. In this study, the data were pre-processed in the HEC–GeoHMS software and was later used as input in the HEC–HMS hydrological model. The HEC–GeoHMS along with the Arc-Hydro tool was used to develop Agree streams for creating river network and DEM data were used for delineating the basin and other characteristics that describe the drainage pattern of the basin. A total of four sub-basins were created according to the meteorological stations present in the study area. The Arc-Hydro geoprocessing tool used for creating inputs for the HEC–HMS model has been summarized by Li (2014) and Baumbach et al. (2015).

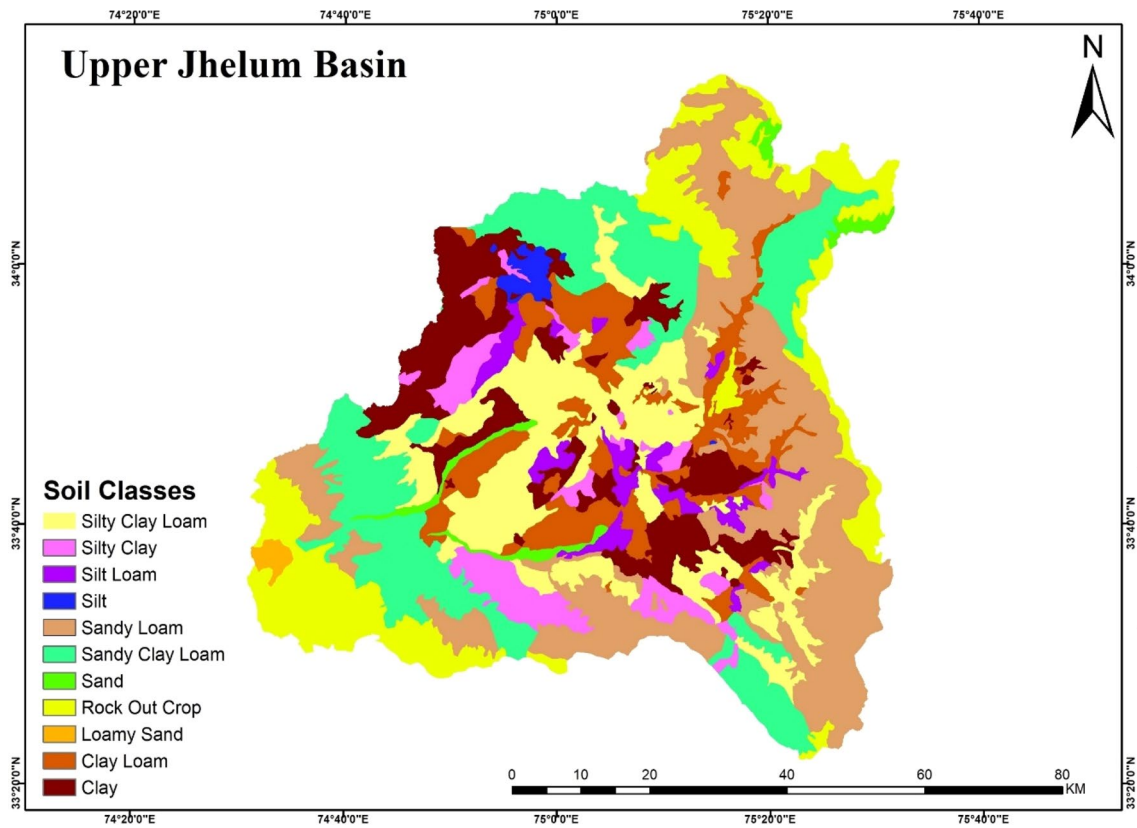


Fig. 5 Major soil groups in upper Jhelum basin

Table 2 Description of soil textural classes in upper Jhelum basin

S. no.	Soil texture	Area (km ²)	% Area
1	Silty clay loam	771.62	14.24
2	Sandy loam	1278.10	23.59
3	Sandy clay loam	924.67	17.07
4	Silty loam	162.36	3.00
5	Clay	571.00	10.54
6	Rock out crop	741.09	13.68
7	Sand	81.12	1.50
8	Clay loam	545.95	10.08
9	Silty clay	273.91	5.06
10	Silt	44.58	0.82
11	Loamy sand	22.66	0.42
	Total	5417.06	100

HEC–HMS file preparation

The HEC–GeoHMS plugin embedded in ArcGIS 10.5 was used to link the files prepared for running the HEC–HMS model. In, HEC–GeoHMS the project file was created and converted to a suitable format easily understood by the concerned hydrological model. The detailed procedure has been

described in the User’s manual (US Army Corps of engineers 2013).

HEC–HMS model description

The HEC–HMS is an open-source model easily used with the ArcGIS software for effective and efficient simulation of most hydrological activities (Mohammed et al. 2011; Kabiri et al. 2013; Ghorbani et al. 2016). The HEC–HMS schematic is shown in Fig. 6. The HEC–HMS model has been divided into four groups based on its simplicity in representing the water cycle: (1) basin model; (2) meteorological model; (3) control specifications; (4) input data. The basin model comprises information about the physical characteristics of the model such as sub-basin area, river network, junctions, reservoirs, source, and sink. The meteorological model contains information about the precipitation data. The control specifications encompass information relevant to the timing of the model like start and end date, start and end time, and the time interval between storm events. The input data comprise the boundary conditions and the input parameters for the basin and the meteorological components of the model. The inputs used for the study constitute precipitation data, observed streamflow data, and different characteristics of

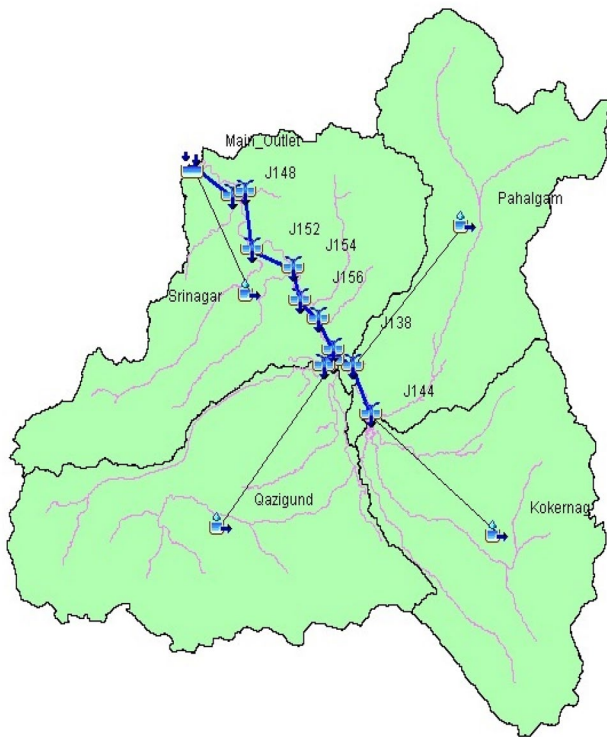


Fig. 6 HEC-HMS schematic

the basin (land use/cover, soil data, and slope) generated from the HEC-GeoHMS tool (Belayneh et al. 2020; Kastali et al. 2022). The modeling framework of HEC-HMS model is shown in Fig. 7.

Loss method

The loss method is used to perform calculations for the actual infiltration that is occurring within the sub-basin. There are a total of twelve loss methods and among them some are designed for event-based and some for continuous simulation modeling. All these methods work on the principle of conservation of mass, i.e., the total amount of precipitation received is equal to the summation of the infiltrated water and the precipitation left on the surface. In this study, continuous modeling was performed using the SMA.

SMA loss method

SMA is a loss method that is used to simulate the behavior of the hydrological system for both dry and wet weather seasons. The SMA algorithm is developed after Leavesley's Precipitation-Run-off Modelling System (1983) and has been described by Bennett and Peters (2000) in detail. The SMA algorithm makes use of three storage layers to simulate the moisture content changes occurring throughout the soil profile. It is used with the canopy method and surface method

to extract water from the soil layers and hold water on the soil surface, respectively, and aids in continuous simulation. The model works on the principle of simulating the movement of water on the soil surface and storing water on vegetation, through the soil profile and groundwater layers. The model estimates the surface run-off, sub-surface run-off, groundwater flow, deep percolation, and ET losses over the entire basin when precipitation and ET are given. In the SMA model, the rate of inflow and outflow of water and capacities of different soil storage layers control the volume of water added or lost to each of the storage components. These storage components vary continuously during the process of simulation both during and between storm events. The different layers for storage in the SMA model comprise canopy-interception storage, surface interception storage, soil profile storage, and groundwater storage. The flow component in the SMA model computes inflow, outflow, and flow of water between different storage layers and can be represented as precipitation and infiltration. The components of the SMA loss method are shown in Fig. 8.

Transform method

The actual surface run-off calculations performed in a sub-basin are done by the transform method. There are a total of nine methods that comprise several unit hydrograph methods, a linear semi-distributed model, a two-dimensional diffusion wave method, and a kinematic wave method. In the present study, the Clark unit hydrograph transform method was used to compute the surface run-off occurring in the basin.

Clark unit hydrograph transform method

It is a synthetic unit hydrograph method that takes into consideration the time-area curve to develop the translation hydrograph resulting from the abrupt precipitation. The resultant unit hydrograph is routed through the linear reservoir to consider the storage attenuation effects occurring in the basin. The standard Clark unit hydrograph method calculated the time of concentration (maximum travel time in the basin) and is an important factor in developing the translation hydrograph. The storage coefficient is another parameter that describes the storage effects. It is a dimensionless ratio of the storage coefficient and summation of storage coefficient and the time of concentration. The storage coefficient remains constant over a region. The time of concentration and storage coefficient was estimated using the following equations:

$$T_c = \frac{t^{0.8}}{1140Y^{0.5}}(S + 1)^{0.7}, \quad (5)$$

$$S = \left(\frac{1000}{CN} \right) - 10, \quad (6)$$

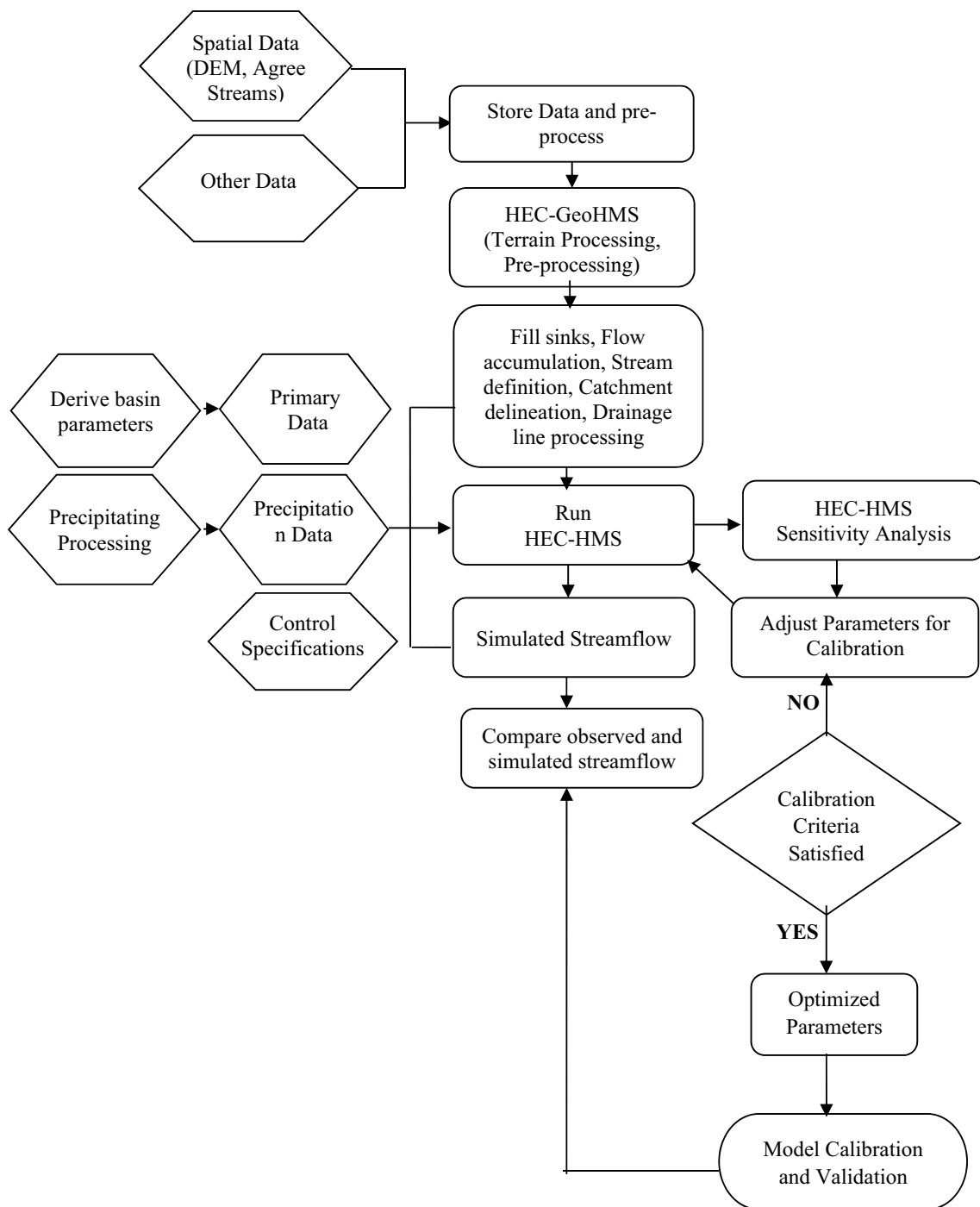


Fig. 7 HEC-HMS modeling framework

$$R = (T_c + R) \times 0.65, \tag{7}$$

where T_c represents the time of concentration (h) l represents the flow length (ft), Y is the average watershed land slope (%), S is the maximum retention potential (in), CN is the curve number, R is the storage coefficient (h).

Baseflow method

The sub-surface calculations are done by the baseflow method. There are a total of six baseflow methods used in the HEC-HMS model. Among these methods, some are used for event modeling and some for continuous

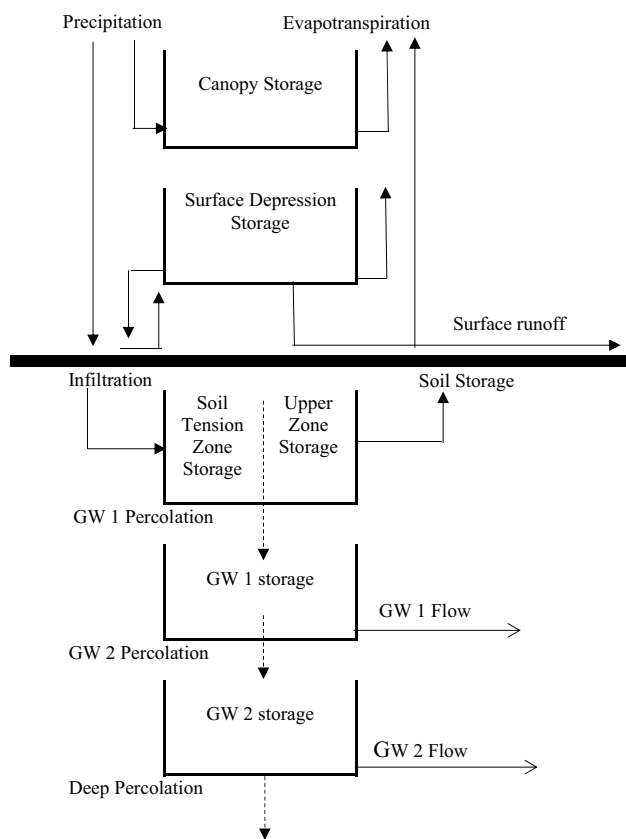


Fig. 8 Flow chart showing the components of the SMA loss method

modeling. In this study, the linear reservoir baseflow method was selected to carry out the process of simulation.

Linear reservoir baseflow

The linear reservoir baseflow method computes the baseflow recession by using a linear reservoir and only this baseflow method works on the principle of mass conservation in a basin. The processes of percolation and infiltration act as the inflow for the linear reservoirs. There can be one, two, or three baseflow reservoirs and when used with the SMA loss method, the number of reservoirs should be consistent with the groundwater layers.

Routing method

The routing method when used with the storage method simulates the actual storage in a basin in the HEC–HMS model. There are several routing methods but in the current study, Lag routing was used for continuous simulation of the model.

Lag routing method

The lag routing method is the most simplified routing method for hydrological processes in the HEC–HMS model. The method does not represent the attenuation or diffusion of wave processes but only represents the translation of flood waves. This method is best suited for steep slopes and small streams having travel time that is predictable and does not alter with changing conditions. Parameters required to carry out this routing procedure are initial conditions and the lag time. Lag time is the travel time taken by the inflow hydrograph to get translated while passing through the reach. The equation for calculating the lag time is given below:

$$Lag = 0.6Tc, \quad (8)$$

where *Lag* is the lag time in minutes.

Data inputs for developing the HEC–HMS SMA model

The HEC–GeoHMS tool was used to create the raster grids to set up and configure the HEC–HMS SMA model. In the SMA algorithm, the loss method was used to carry out the continuous simulation of run-off in the upper Jhelum basin. SMA loss method takes into consideration the five storage layers to describe the movement of water from the surface to the sub-surface soil profile and before the beginning of the simulation process, the values of these layers were specified as the percentage of water in the respective storage layer. The layers were converted into raster datasets and were used as the input for developing the HEC–HMS SMA model. The raster datasets created were (i) maximum canopy storage, (ii) maximum surface storage grid, (iii) maximum soil infiltration grid, (iv) maximum soil percolation grid, (v) soil tension storage grid, (vi) maximum soil storage grid, (vii) Groundwater 1 (GW1) maximum storage grid, (viii) Groundwater 2 (GW2) maximum storage grid, (ix) GW1 maximum percolation grid, (x) GW2 maximum percolation grid. Raster datasets from (i) to (vi) were extracted from the land use/cover grid and FOA soil database. Raster datasets (vii) and (viii) had constant values. The value for the raster (ix) dataset was considered to be equal to raster (iv) and the value for raster (x) was assigned during the calibration process of the HEC–HMS model as it is an extensively conceptual parameter.

The maximum canopy storage is the amount of water that remains on the leaves and overlapping branches before the beginning of the surface flow. The canopy grid raster was created from a land cover grid generated according to NLCD classes. The different land use classes have different canopy-interception values (Table 3) and the appropriate values for

Table 3 Canopy interception values

Type of vegetation	Canopy interception	
	Inches	Millimetre
General vegetation	0.05	1.270
Grasses and deciduous trees	0.08	2.032
Trees and coniferous trees	0.1	2.540

Fleming and Neary (2004)

the study areas were chosen from the table. The maximum canopy raster map is shown in Fig. 9. For each component of the soil layer, average saturated hydraulic conductivity (*ksat_avg*), saturated hydraulic conductivity for layer 1 (*ksat_Layer1*), average soil porosity (*wsat_avg*), average field capacity (*wthirdbar_avg*), depth from the top layer of the soil surface to bottom layer (*hzdepb*) and weighted slope of each map unit were calculated. The percentage of the particular map unit occupied by the specific component was displayed by the component percent (*Compct*). The maximum surface depression storage is the maximum depth of water that soil can store in depression areas before the beginning of the surface run-off process and was calculated by multiplying the slope of each map unit by the *Compct* and summing the value for each map unit. The map for maximum surface depression storage is shown in Fig. 10. The values

for the surface depression storage for different surfaces are shown in Table 4 and according to the weighted slope value appropriate storage depression values were chosen. There exists only one surface storage value for each map unit. The maximum infiltration rate is the maximum rate at which the water is infiltrated into the soil. The maximum infiltration rate was calculated by multiplying and summing the values of *Compct* and *ksat_Layer1* of each map unit and the map for the same is shown in Fig. 11. The maximum soil profile storage is the capacity of the soil to store water in the pores and was estimated by multiplying and summing the *wsat_avg* and *hzdepb*. The map for maximum soil profile storage is shown in Fig. 12. The tension storage zone is where the water is attached to the soil particles and is lost only to ET. The maximum tension zone was calculated by multiplying and summing *wthirdbar_avg* and *hzdepb* for each map unit. The map for the maximum tension storage zone is shown in Fig. 13. The percolation rate of water in the soil is the time taken by the water to flow through the sub-surface layers. The percolation rate for each component was calculated by multiplying and summing *ksat_avg* and *Compct* for each map unit. Raster grids sets were created for all these components and were assigned to the sub-basin parameters from rasters and average parameter values were calculated for each sub-basin. The map for the maximum percolation rate is shown in Fig. 14. The maximum soil percolation rate was

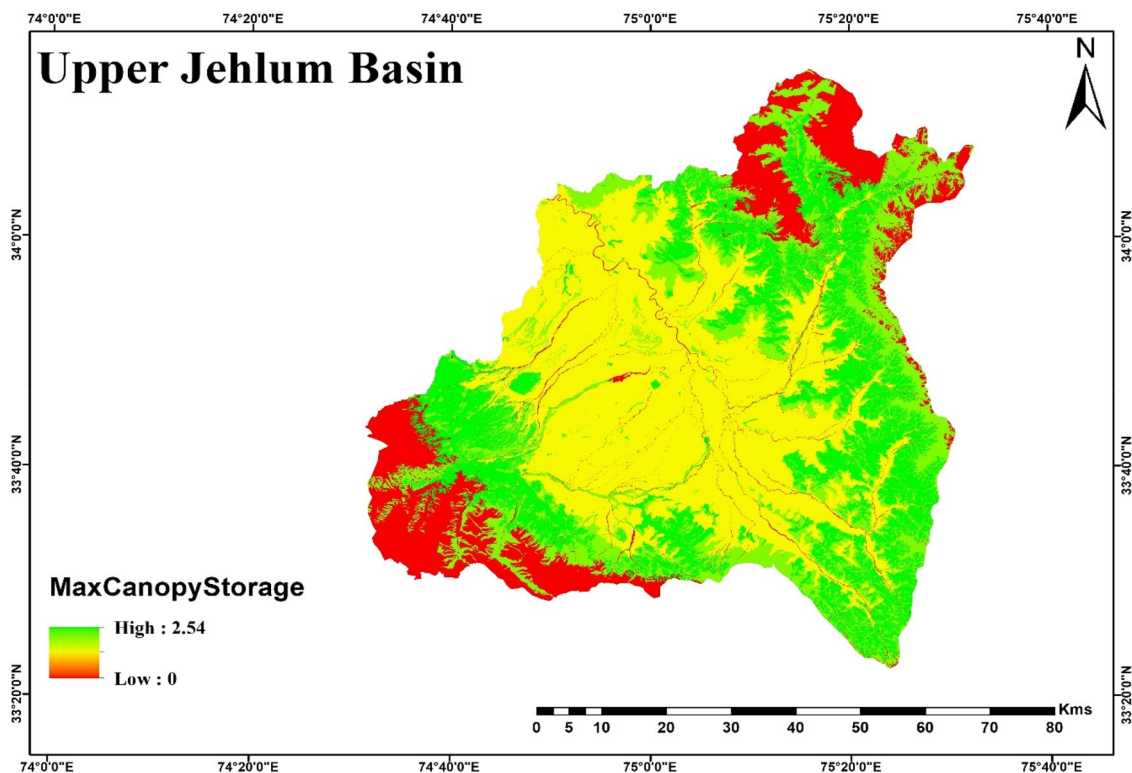


Fig. 9 Maximum canopy storage map

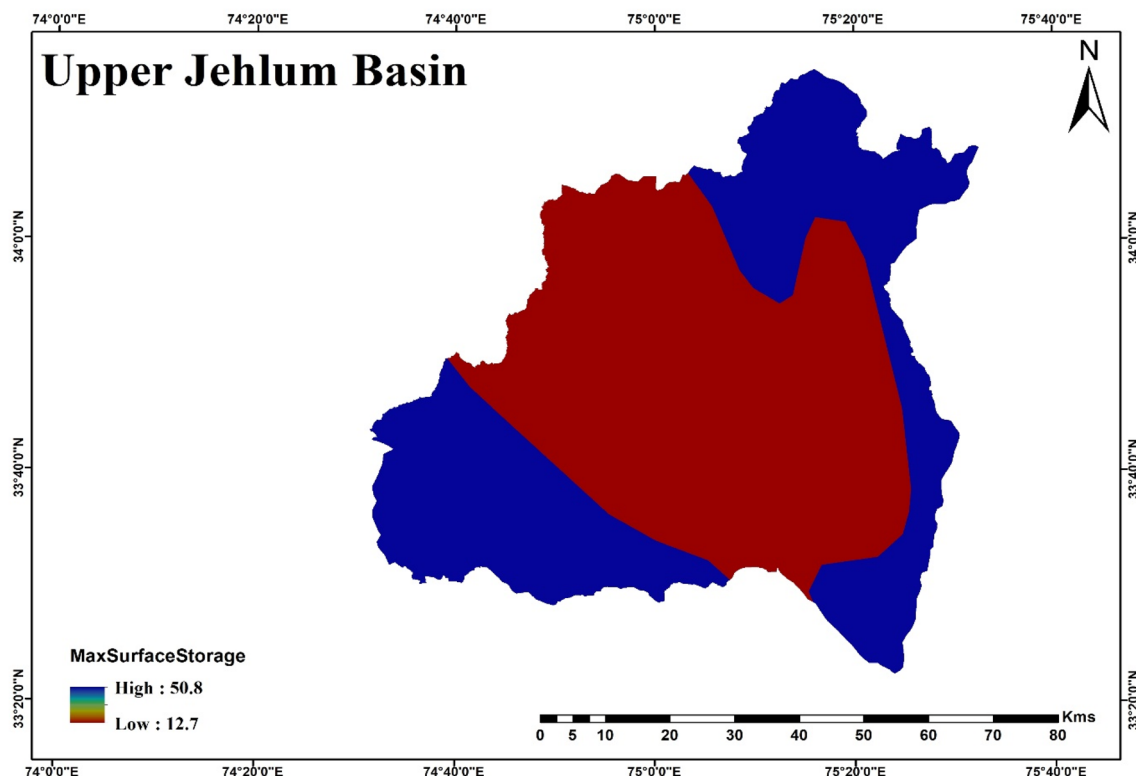


Fig. 10 Maximum surface depression storage

Table 4 Surface depression storage values

Description	Slope (%)	Surface storage	
		Inches	Millimetre
Paved impervious areas	NA	0.125–0.25	3.18–6.35
Flat, furrowed land	0–5	2.00	50.8
Moderate to gentle slopes	5–30	0.25–0.50	6.35–12.70
Steep, smooth slopes	> 30	0.04	1.02

Fleming and Neary (2004)

also used to create the GW1 maximum percolation grid. SMA parameters, data source, and estimation methods are described in Table 5.

Parameters estimated from upper Jhelum streamflow data

The point of inflection on the recession curve of a hydrograph is the point where the surface flow does not contribute anymore to the surface run-off and the recession curve shows the contributions only from interflow and groundwater flow after this point (Fig. 15). The value of the recession constant of the streamflow is calculated by the recession analysis of the historical stream flow data. The recession curve of the hydrograph or the receding limb of the hydrograph

is represented by the following equations (Singh and Jain 2015):

$$Q = Q_0 K^t \tag{9}$$

$$\alpha = -\ln K \tag{10}$$

where Q is the discharge (m^3/s), Q_0 is the initial discharge (m^3/s), K is the recession constant.

The recession constant account for three different types of components that pertain to three types of storage and was represented as shown in the following equation:

$$K = K_s \cdot K_i \cdot K_b \tag{11}$$

where K_s is the recession constant for surface storage. K_i is the recession constant for interface, K_b is the recession constant for baseflow.

The recession constant was plotted against the discharge on a log-scale on a semi-log paper and was calculated from the historical data of streamflow. The storage at the time, t in the basin was estimated by the following equation:

$$S_t = \left(\frac{Q}{\alpha} \right) \tag{12}$$

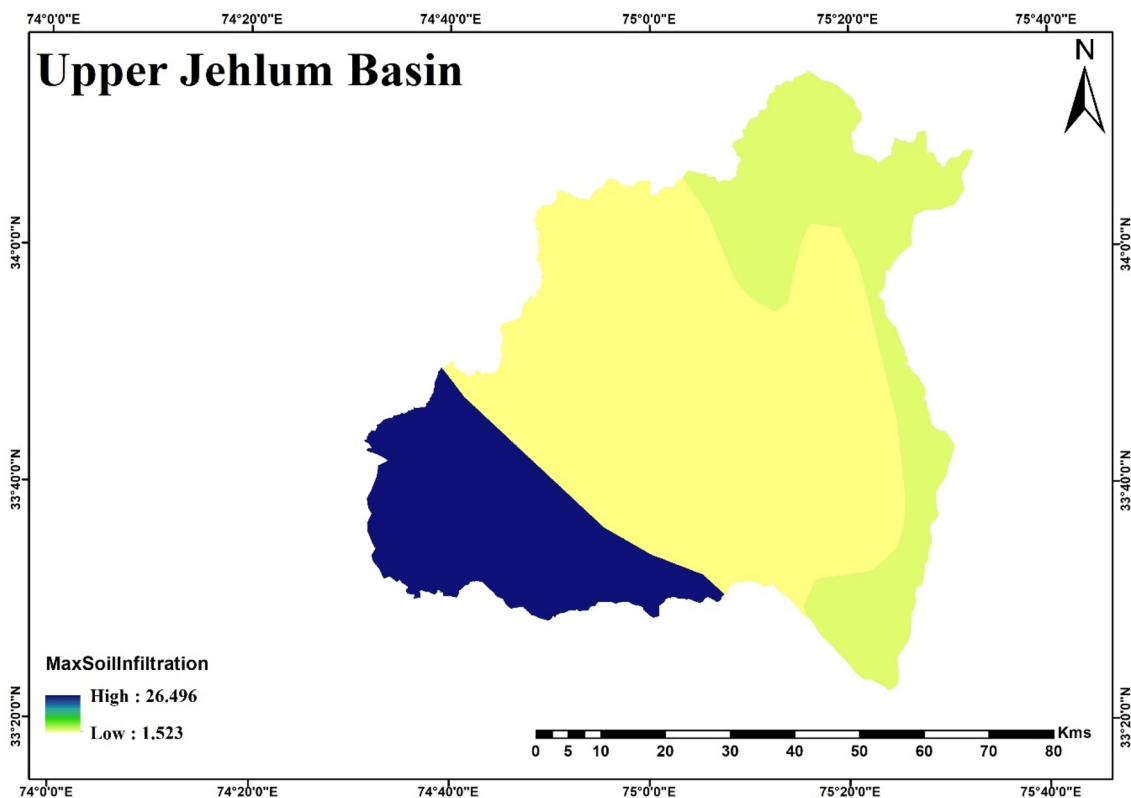


Fig. 11 Maximum infiltration rate

The hydrographs were selected from various seasons and from different storm events where there was no rain for some days after the peak flow was attained and the storage parameters and recession constant were evaluated.

Calibration and validation of the HEC–HMS model

The hydrological model needs to undergo the process of calibration and validation using the actual streamflow values to obtain the desired and reliable outputs. The observed streamflow was compared with the simulated streamflow for evaluating the goodness of fit and to suggest whether the hydrological model can predict the streamflow efficiently at three discharge stations (Ram Munshi Bagh, Sangam, and Rambiara). The HEC–HMS hydrological model was run for a period of 20 years (2000–2019) where 3 years were used as the warm-up period for the model. The model was calibrated for a period of 12 years from 2003 to 2014 and validated for a period of 5 years from 2015 to 2019. The optimization trials were carried out through the auto-calibration process and the values of the input parameters were also adjusted using the manual calibration of the HEC–HMS model and the set of optimized parameters was obtained. The optimized parameters were used further to perform the validation of the model and evaluate the goodness of fit for the simulated and the observed

streamflow. The HEC–HMS hydrological model performance analysis incorporated the assessment of goodness of fit in both observed and simulated discharge using performance indicators like coefficient of determination (R^2), Nash–Sutcliffe efficiency (NSE), Kling–Gupta efficiency (KGE), percent bias (PB), mean absolute error (MAE), and root mean square error (RMSE). The equations of these six statistical indices have been described below:

$$R^2 = \frac{\left[\sum_{i=1}^N (Q_{obs} - \bar{Q}_{obs})(Q_{sim} - \bar{Q}_{sim}) \right]^2}{\sum_{i=1}^N (Q_{obs} - \bar{Q}_{obs})^2 \sum_{i=1}^N (Q_{sim} - \bar{Q}_{sim})^2}, \tag{13}$$

$$NSE = \frac{1 - \sum_{i=1}^N (Q_{obs} - Q_{sim})^2}{\sum_{i=1}^N (Q_{obs} - \bar{Q}_{obs})^2}, \tag{14}$$

$$KGE = 1 - \sqrt{(r - 1)^2 + (\alpha - 1)^2 + (\beta - 1)^2}, \tag{15}$$

$$PB(\%) = 100 \times \frac{\sum_{i=1}^N (Q_{obs} - Q_{sim})}{\sum_{i=1}^N Q_{obs}}, \tag{16}$$

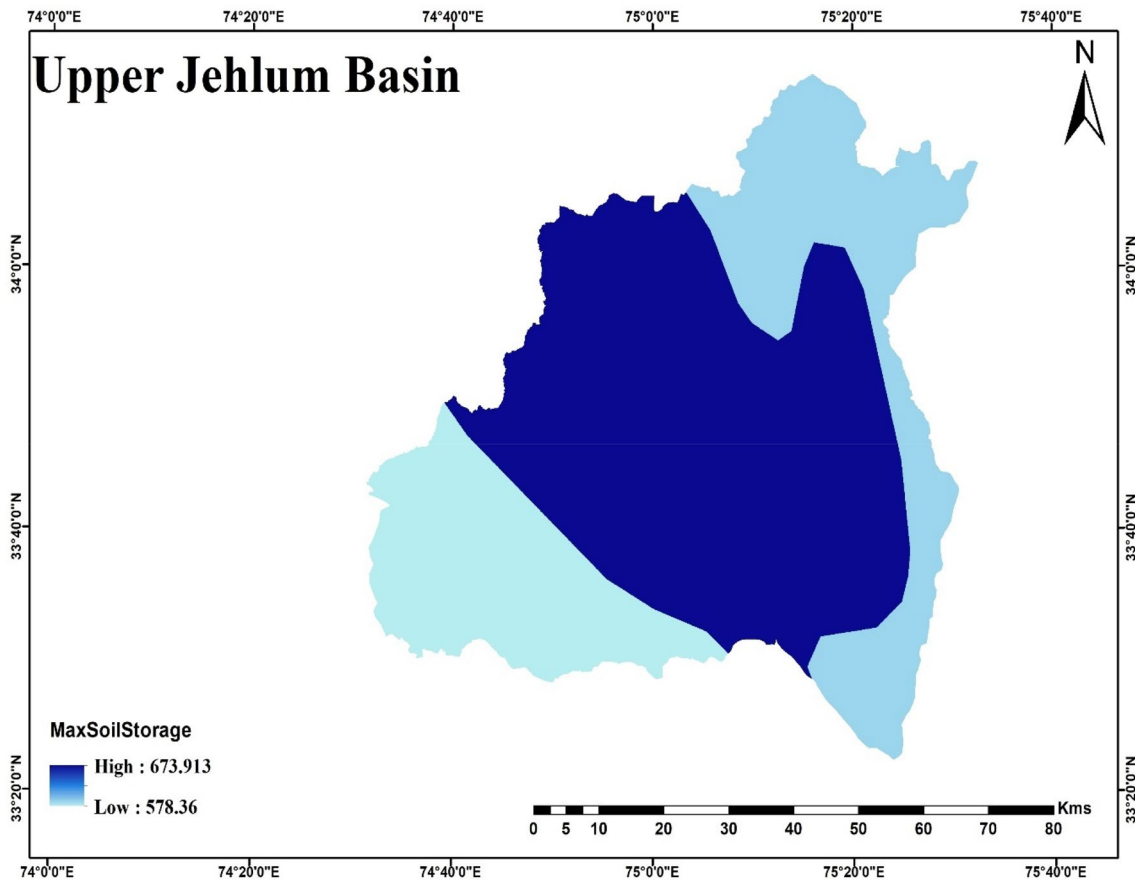


Fig. 12 Maximum soil profile storage

$$\text{MAE} = \frac{1}{N} \sum_{i=1}^N |Q_{\text{obs}} - Q_{\text{sim}}|, \quad (17)$$

$$\text{RMSE} = \sqrt{\frac{1}{N} \sum_{i=1}^N (Q_{\text{obs}} - Q_{\text{sim}})^2}, \quad (18)$$

where Q_{obs} is the observed value, \bar{Q}_{obs} is the mean observed value, Q_{sim} is the simulated value and \bar{Q}_{sim} is the mean simulated value, r is the linear correlation between observed and simulated values, α is a measure of flow variability error and β is a bias term.

Sensitivity analysis

The sensitivity analysis is a vital component of the hydrological modeling that aids in the identification of the most sensitive parameter affecting the basin hydrology. The set of optimized parameters comprises the influential and the non-influential parameters. A small change in the value of the sensitive parameter leads to drastic changes in the model simulated results. The sensitivity analysis of the SMA algorithm parameters was

conducted using the OAT method where each input parameter value was varied by $\pm 10\%$ while keeping the remaining parameters at their default values.

Results

The total area covered by the upper Jehlum river basin is 5417.1 km^2 with the highest and lowest elevations of 5308 m and 1561 m, respectively, the total length of 88.90 km, mean width of 60.90 km, and perimeter equal to 368.60 km. The basin constitutes dendritic, trellis, and parallel to the subparallel type of drainage pattern. The basin characteristics such as sub-basin area, perimeter, relief, length, minimum and maximum elevation, number of micro watersheds, and length of the main channel are represented in Table 6.

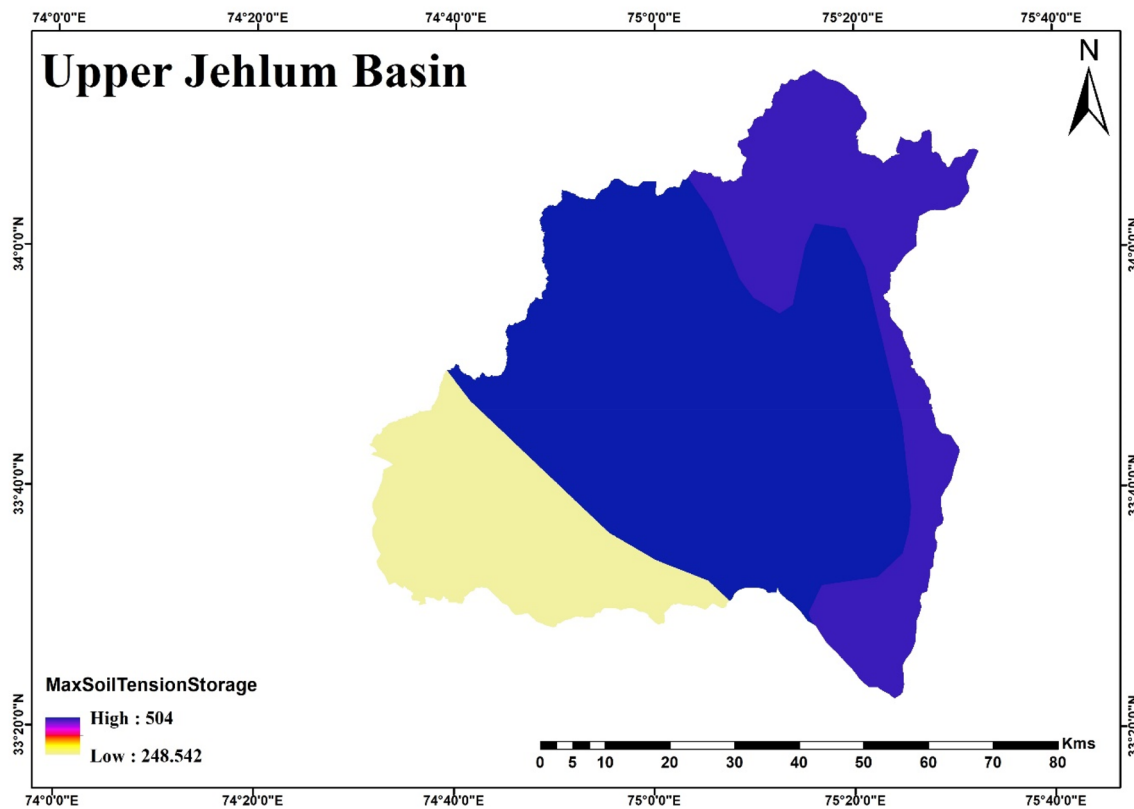


Fig. 13 Maximum soil tension storage zone

Upper Jhelum basin hydroclimatic conditions

Temperature

The temperature data were studied for a period of 20 years ranging from 2000 to 2019. The values over four meteorological stations were averaged and the mean minimum and maximum temperature (T_{\min} , T_{\max}) were recorded (Fig. 16). The results show that the mean annual T_{\max} in the basin ranges from 17.0 to 20.5 °C with a mean value of 18.9 °C. Similarly, the mean annual T_{\min} recorded ranges from 3.4 to 7.7 °C with an average value of 6.1 °C. The maximum temperature was recorded in July where T_{\max} and T_{\min} were 27.7 °C and 16.1 °C, respectively. The lowest temperature (sub-zero) was recorded in January when the winter season in the basin starts to begin. Minimum and maximum temperature values for January were as 6.9 °C and – 3.2 °C, respectively.

Precipitation

The evaluation of precipitation averaged over four observed meteorological stations revealed that the average annual rainfall for the period of 2000–2019 was 1684.1 mm

(Fig. 17). The lowest and highest average annual rainfall values were recorded to be 654.3 mm in 2000 and 1477.8 mm in 2014, respectively. The lowest precipitation was recorded in November averaging 44.5 mm and the highest precipitation of 130.3 mm was received in March.

Streamflow

The changes in the streamflow of the upper Jhelum basin at three discharge stations are shown in Fig. 18. Sangam station showed the maximum peak discharge (3465.3 cumecs), followed by Ram Munshi Bagh (2634.6 cumecs) and Rambiara (1716.3 cumecs). The maximum annual peak flow was recorded for the year 2014 (flood year) for all the three gauging stations. The minimum annual peak flow discharge for Sangam was 2079.9 cumecs, 1160.4 cumecs for Ram Munshi Bagh and 600.9 cumecs for Rambiara.

Parameterization and sensitivity analysis

The basic step in the process of calibration is the identification of the influential parameters that govern the streamflow conditions. Sensitivity analysis of the HEC–HMS model was carried out by OAT method prior to calibration and validation concerning SMA parameters. The sensitivity analysis of

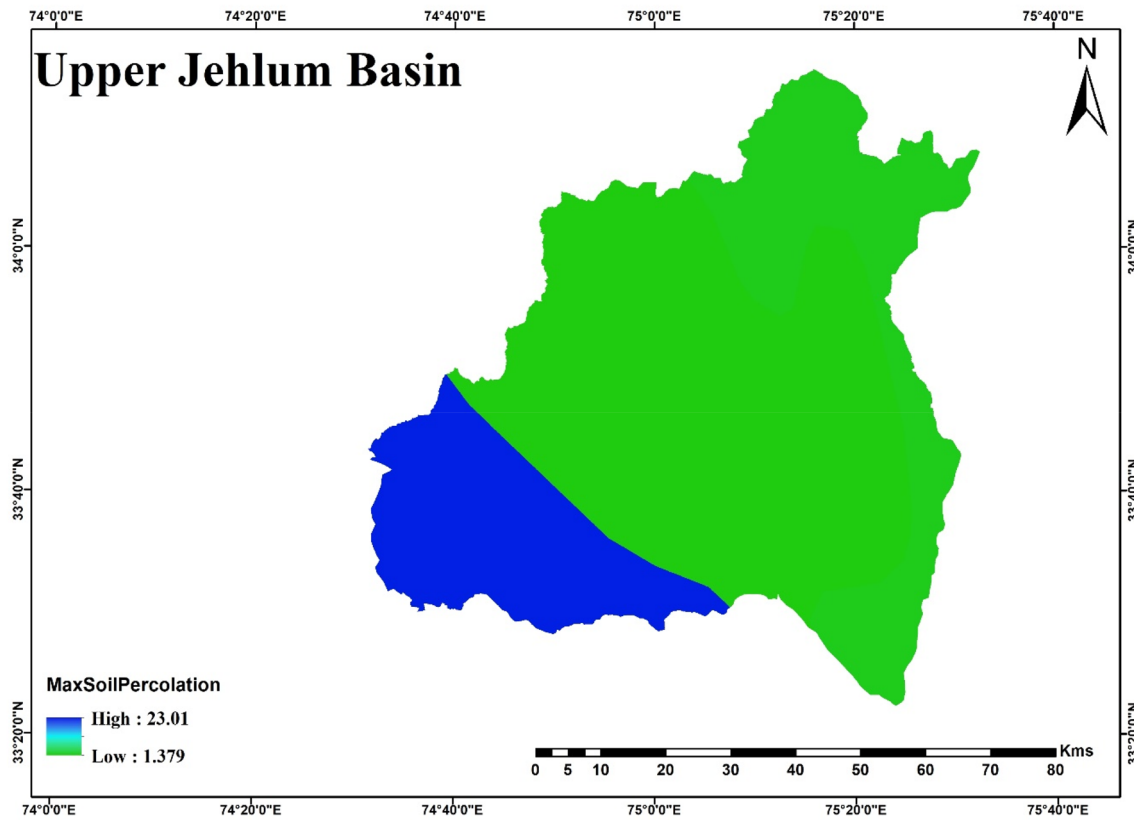


Fig. 14 Maximum soil percolation rate

Table 5 SMA parameters, data, and estimation methods

Parameters	Data source	Initial condition	Method
Canopy storage (mm)	Soil database	Canopy storage (%)	Calibration
Surface storage (mm)	Soil database	Canopy storage (%)	Calibration
Max infiltration rate (mm/h)	Soil database	Soil storage (%)	Calibration
Max soil storage (mm)	Soil database	GW1 filled storage (%)	Calibration
Soil tension storage (mm)	Soil database	GW1 filled storage (%)	Calibration
Soil percolation rate (mm/h)	Soil database		
GW1 storage (mm)	Base flow		
GW1 max percolation rate (mm/h)	Soil database		
GW1 storage coefficient (h)	Calibration		
GW2 storage (mm)	Base flow		
GW2 max percolation rate (mm/h)	Calibration		
GW2 storage coefficient (h)	Calibration		

thirteen SMA parameters was analyzed by separately varying each parameter from -50% to $+50\%$ in increments of 10% . The percent change in simulated volume was then plotted against the percent change in variation of each parameter (Fig. 19). From the analysis, it was found that soil storage was the most sensitive parameter followed by tension zone storage and soil percolation. GW2 coefficients, percolation and storage were found to be the least sensitive parameters

while carrying out the process of calibration. The ranking of parameters according to their sensitivity concerning the change in simulated volume is shown in Table 7.

HEC–HMS model calibration and validation

The HEC–HMS model streamflow simulation in the upper Jhelum basin was carried out at selected three gauging

Fig. 15 Hydrograph representing contributions from GW1 (Interflow) and GW2 (Baseflow)

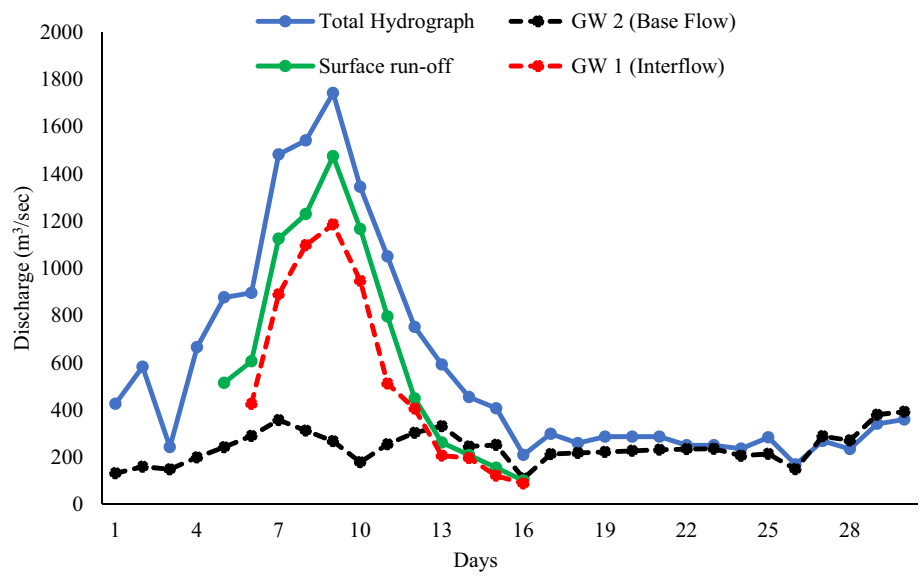


Table 6 Basic morphometric parameters of the upper Jhelum basin

Sub-basin	Area (km ²)	Perimeter (km)	Length (km)	Maximum elevation (m)	Minimum elevation (m)	Basin relief (km)	Length of main channel (km)	No of micro watersheds
Veshav	1014.8	161.4	44.1	4564.0	1559.0	3.1	78.6	74
Rambiara	872.6	167.7	58.7	4625.0	1527.0	3.2	76.0	41
Romushi	365.0	122.0	47.3	4651.0	1577.0	2.3	54.0	09
Sandran	365.2	118.3	47.1	4065.0	1583.0	2.5	53.0	16
Bringi	505.4	135.2	40.6	4351.0	1582.0	2.9	53.0	49
Lidder	1267.2	222.6	53.8	5047.0	1535.0	3.9	82.2	98
Kuthar	328.8	89.98	35.5	4300.0	1501.0	2.8	39.0	38
Arapal	539.0	96.7	30.8	4239.0	1495.0	2.9	38.4	53

Fig. 16 Time series of mean maximum and minimum temperature along with trend line

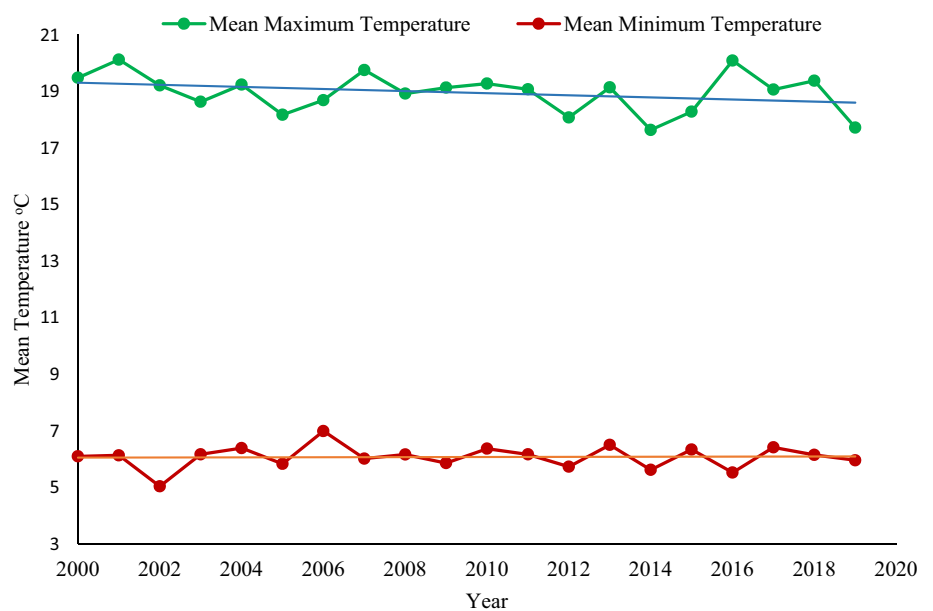


Fig. 17 Annual precipitation along with trend line

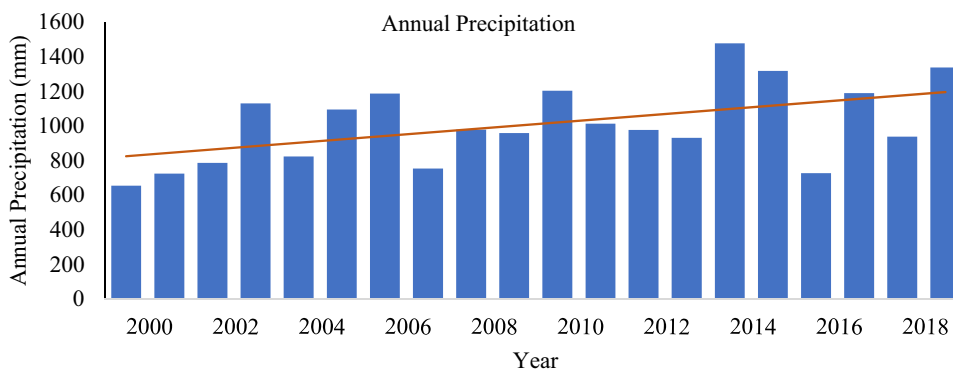


Fig. 18 Time series of stream-flow at multiple gauging sites along with trend lines

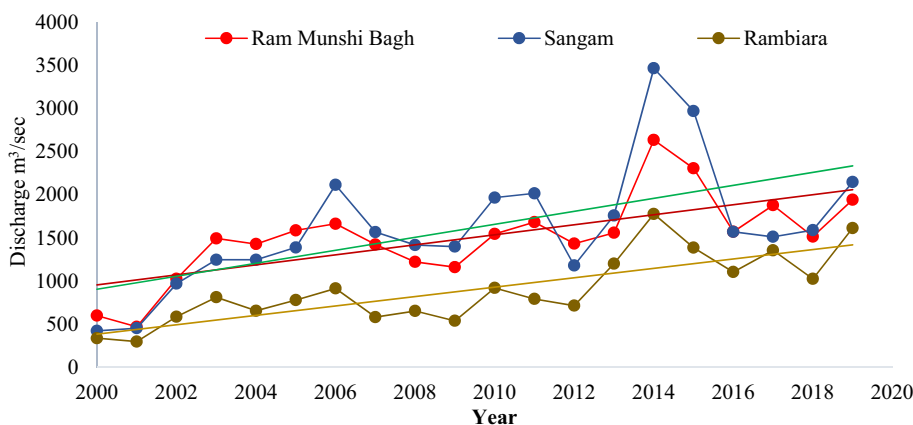
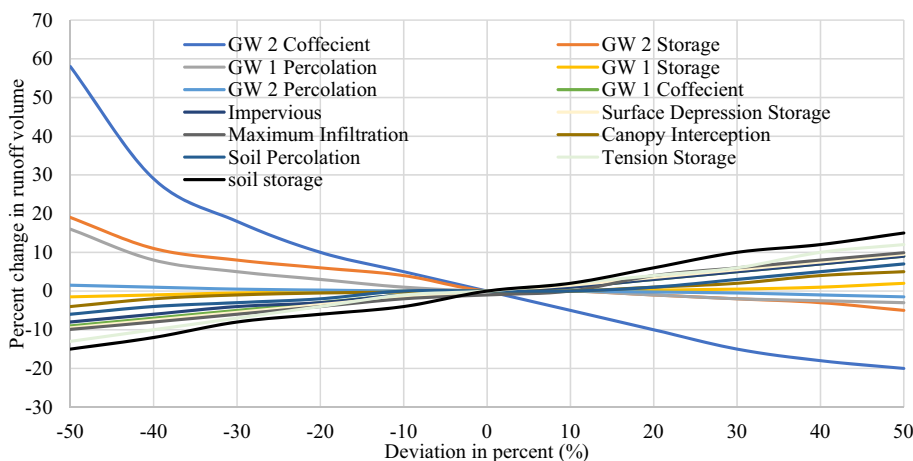


Fig. 19 Sensitivity analysis of HEC–HMS model parameters



stations for a period of 20 years (2000–2019) using 3 years as the warm-up period. The calibration of HEC–HMS was performed from 2003 to 2014 to estimate daily run-off in the basin. The auto-calibration methods embedded in the HEC–HMS model were used to first calibrate the input parameters and then these parameters were further fine-tuned to obtain the best-optimized values using manual calibration procedures. After successfully calibrating the model, the optimized parameters generated were utilized

to simulate the model for the validation period. Table 8 shows the various optimized parameter values for the study area. The HEC–HMS model was validated for a period of 5 years (2015–2019). The optimization of the model parameters was performed based on six objective functions. The statistical evaluation of the model at three gauging stations for the calibration period is presented in Table 9. The values of R^2 , NSE, and KGE for Ram Munshi Bagh station were 0.808, 0.793, and 0.866 while the

Table 7 Ranking of model parameter as per the sensitivity analysis

Parameters	Ranking
Soil storage	1
Soil tension storage	2
Soil percolation	3
Maximum infiltration	4
GW1 storage	5
GW1 percolation	6
Canopy storage	7
Surface depression storage	8
Impervious	9
GW1 coefficient	10
GW2 storage	11
GW2 percolation	12
GW2 coefficient	13

computation of these coefficients for Sangam and Rambiar station were 0.783, 0.753, 0.871, and 0.793, 0.788, 0.816, respectively. Percent bias, MAE, and RMSE represented the errors in the model simulation and for Ram Munshi Bagh these errors were estimated to be 7.9%, 31.462, and 43.798 whereas, these errors were 2.7%, 49.718, and 59.628 for Sangam and 5.1%, 19.578 and 26.644 for Rambiar station.

The statistical performance of the HEC–HMS model during the validation period is summarized in Table 10. The results reveal that the performance of the validation period is in similitude to the calibration period. The same statistical coefficients were used for the validation period as used in the calibration period. The values of R^2 for validation were found to be 0.832 for Ram Munshi Bagh station, 0.805 for Sangam, and 0.833 for Rambiar station. NSE values obtained were 0.819 for Ram Munshi Bagh, 0.767 for Sangam, and 0.819 for Rambiar station, whereas KGE for these three stations were 0.898, 0.864, and 0.807, respectively. The model error evaluators PB, MAE, and RMSE were 5.2%, 36.497, and 49.433 for Ram Munshi Bagh, 4.2%, 49.921, and 63.995 for Sangam, and 6.8%, 32.082 and 39.362 for Rambiar station.

The HEC–HMS model performance was further judged by the graphical comparison between the observed and simulated streamflow values. The hydrograph and the scatter plots for the observed and simulated streamflow for calibration and validation periods for three discharge stations are shown in Figs. 20a–f and 21a–f, respectively. It is evident from the figures that the HEC–HMS model satisfactorily simulates the observed discharge and the model has efficiently represented the peak values in the hydrograph. The highest peak flow value was recorded for the year 2014, the flood year, and was correctly depicted by the model, thus,

Table 8 SMA optimized model parameters for four sub-basins

Parameters	Pahalgam	Kokernag	Qazigund	Srinagar
Max canopy storage (mm)	1.945	1.592	1.6	2.156
Max surface storage (mm)	22.57	33.68	33.21	27.35
Max infiltration rate (mm/h)	22.43	18.89	28.68	17.78
Max soil storage (mm)	650.38	626.75	622.46	640.97
Soil tension storage (mm)	467.78	496.34	466.44	498.65
Soil percolation rate (mm/h)	4.34	3.57	6.45	3.87
GW1 storage (mm)	510	532	515.38	533.69
GW1 max percolation rate (mm/h)	4.3	12.12	3.8	3.4
GW1 storage coefficient (h)	750	780	672	760
GW2 storage (mm)	720	732	714.38	710.03
GW2 max percolation rate (mm/h)	3.5	10.82	3.6	3.1
GW2 storage coefficient (h)	4020	3039	2257	3122

Table 9 Statistical parameters for calibration period (2003–2014) at different gauging stations

S. no.	Statistical parameters	Stations		
		Ram Munshi Bagh	Sangam	Rambiar
	Correlation coefficient (R^2)	0.808	0.783	0.793
	Nash Sutcliff efficiency (NSE)	0.793	0.753	0.788
	Kling Gupta efficiency (KGE)	0.866	0.871	0.816
	Percent bias (P.B)	7.9%	2.7%	5.1%
	Mean absolute error (MAE)	31.462	49.718	19.578
	Root mean square error (RMSE)	43.798	59.628	26.644

Table 10 Statistical parameters for validation period (2015–2019) at different gauging stations

S. no.	Statistical parameters	Stations		
		Ram Munshi Bagh	Sangam	Rambiara
	Correlation coefficient (R^2)	0.832	0.805	0.833
	Nash Sutcliffe efficiency (NSE)	0.819	0.767	0.819
	Kling Gupta efficiency (KGE)	0.898	0.864	0.807
	Percent bias (P.B)	5.2%	4.2%	6.8%
	Mean absolute error (MAE)	36.497	49.921	32.082
	Root mean square error (RMSE)	49.433	63.995	39.362

suggesting that model can be used satisfactorily for any simulation period.

Discussion

The HEC–HMS hydrologic model needs to be calibrated efficiently using SMA parameters before using the model for quantifying the run-off accurately in the upper Jehlum basin. The SMA parameters are mostly related to the soil properties and are required to be calculated more precisely. In this study, some of the soil properties were obtained from the FAO soil database and others were calculated using empirical equations. The results obtained were very satisfactory. The evapotranspiration is the most important factor influencing continuous simulation and was estimated for the entire basin using Thornwaite’s method on a monthly time scale.

During the process of sensitivity analysis carried upon SMA parameters, the soil storage and soil tension storage zone were found to be the most sensitive parameter in the basin. Singh and Jain (2015) used the SMA algorithm of the HEC–HMS hydrological model in the Vamsadhara river basin, India to simulate streamflow and sensitivity analysis showed soil storage as the most sensitive parameter in the basin. Ismael et al. (2017), also used HEC–HMS to perform run-off simulation in Ruiru reservoir catchment. They also found soil storage to be the most sensitive parameter same as our study. Both the studies were found in close agreement with our present study.

The statistical analysis implies that the model performance indicators (R^2 , NSE, and KGE) and model error evaluators (PB, MAE, and RMSE) are close to the expected value of 1 and 0, respectively. Positive values of PB for all the three gauging stations indicate that the flow is underestimated (Gupta et al. 1999). This may be attributed to the fact that the HEC–HMS model does not take into consideration the flows induced from snowmelt in the watershed (Fontaine et al. 2002). The run-off generated from the snowmelt contributes significantly to the streamflow in the upper Jehlum basin, therefore, in the current study, the high flows were not very efficiently determined by the model due to which the flow was underestimated. The low flows

have been appropriately depicted by the model as the base-flow model was used to study the delayed flows in the basin which included groundwater contributions from the basin. The values of the groundwater coefficients and percolation rates were determined from the total hydrograph analysis. The values of the other statistical coefficients reveal that the model shows minimum bias towards calibration as well as validation periods, resulting in good agreement between observed and simulated discharge values at the three gauging stations and further suggests that the hydrological model has been calibrated satisfactorily for the study area. Our study is in agreement with the similar studies carried by other authors in different basins. Roy et al. (2013) used the HEC–HMS model in eastern India for a river basin to calculate various parameters and evaluate the performance of the model. The calibrated and validated model proved to be the best fit for the concerned study area. Shah and Lone (2021) utilized HEC–HMS hydrological model to simulate streamflow in the Sindh watershed, northwest Himalayas. The results showed a good fit between the observed and the simulated streamflow values and proved the hydrological model can be used in the study area for any simulation period. Altaf and Romshoo (2022) used HEC–HMS in five watersheds of the Upper Jhelum Basin in the Kashmir Himalaya, India. The hydrological model was calibrated to estimate the excess-run-off potential in the basin and the model results showed good agreement with the observed streamflow and the flood-vulnerability assessment of the upper Jhelum basin was well corroborated by the observed floodwater levels and the Vishav watershed was found to be the most vulnerable.

Conclusions

The applicability of the HEC–HMS hydrological model for multi-site streamflow simulation using hydrometeorological inputs is explored for the upper Jhelum basin in a hilly terrain of western Himalayas. The HEC–HMS continuous modeling has been performed in the basin using SMA algorithm. The parameters for the SMA model were generated using HEC–GeoHMS, an ArcGIS interface of the

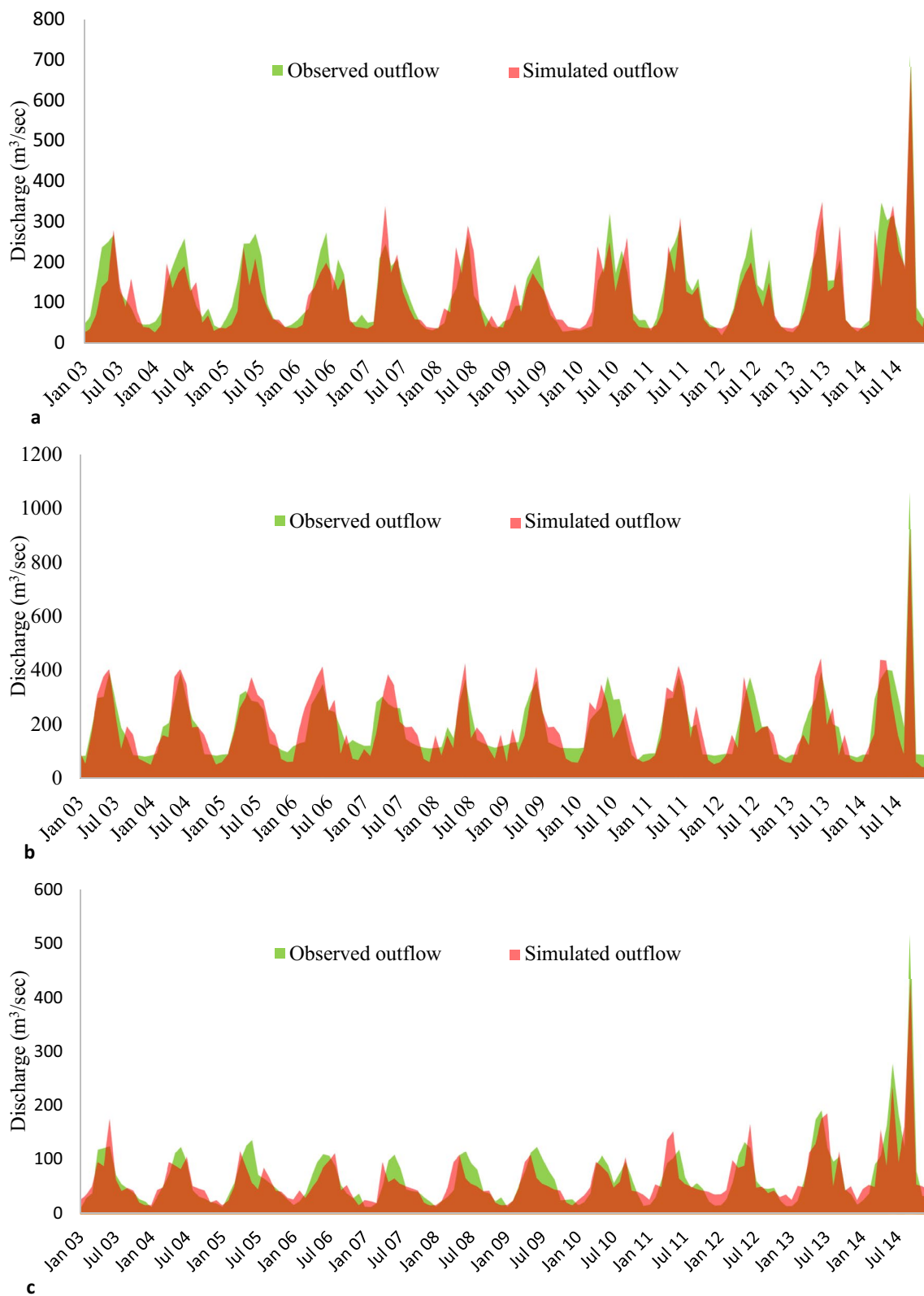


Fig. 20 Observed and simulated flow during calibration period (2003–2014) at **a** Ram Munshi Bagh, **b** Sangam, and **c** Rambiar. The same during validation period (2015–2019) at **d** Ram Munshi Bagh, **e** Sangam, and **f** Rambiar

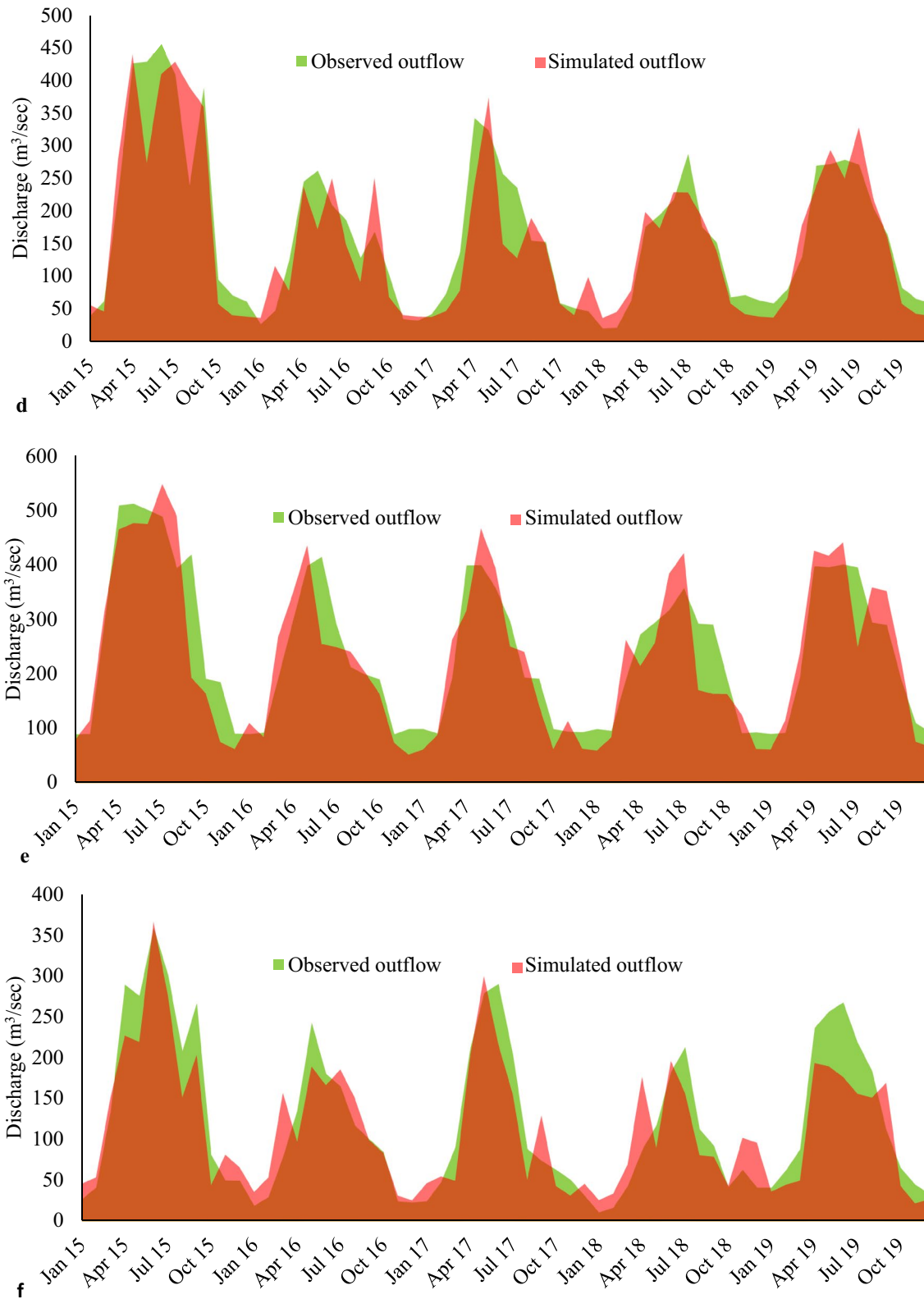


Fig. 20 (continued)

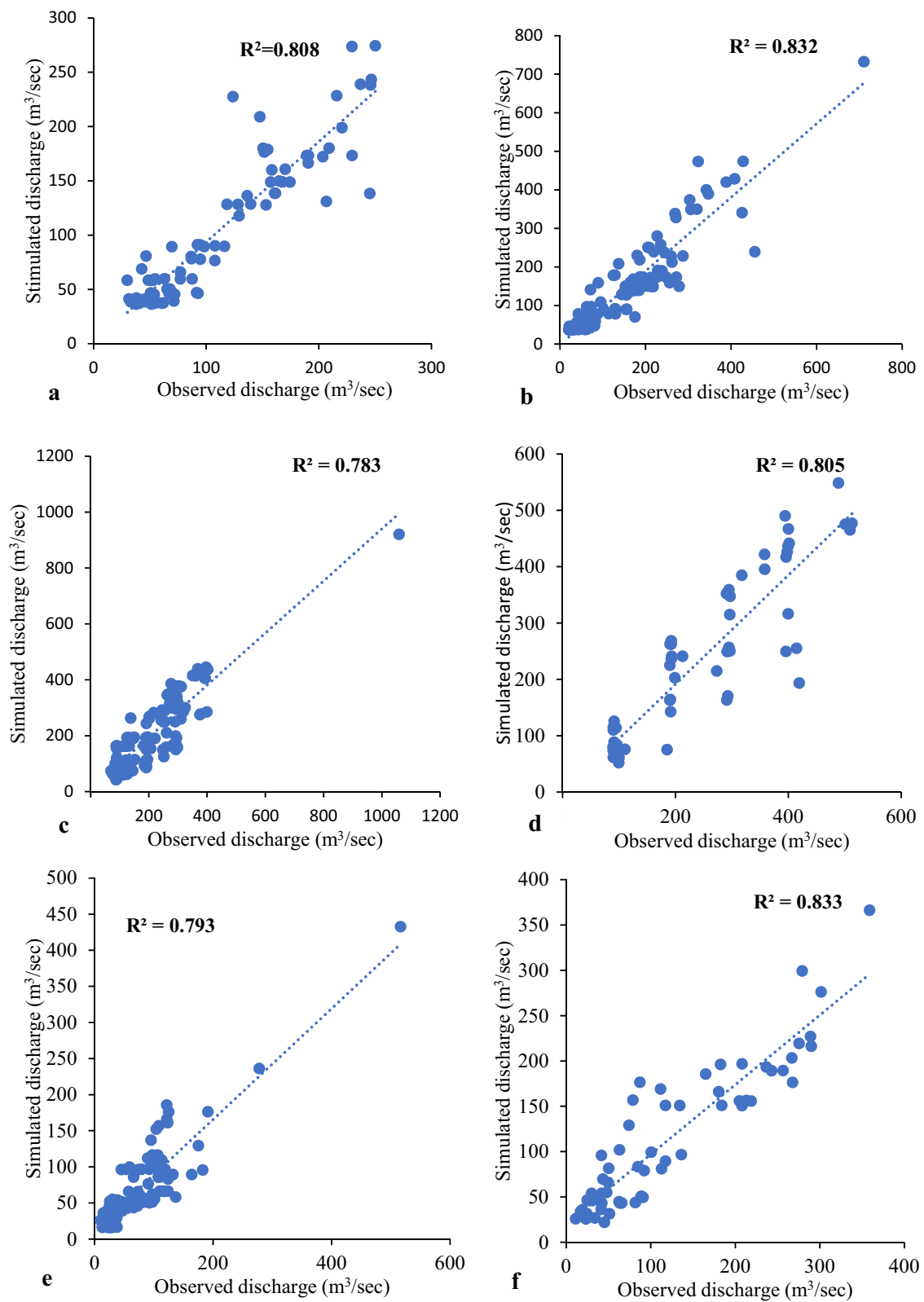


Fig. 21 Scatter plot between observed and simulated streamflow for calibration (a, c, e) and validation (b, d, e) period at Ram Munshi Bagh (a, b), Sangam (c, d), and Rambiara (e, f)

HEC–HMS model. The sensitivity analysis, calibration, and validation were the most important processes to attain runoff simulation results. The sensitivity analysis of the SMA parameters was performed to describe the effect of sensitive parameters on the water movement and its storage in different soil layers. The soil storage was found to be the most sensitive parameter followed by tension zone storage and soil percolation. The HEC–HMS hydrological model was successfully and efficiently calibrated and validated for the upper Jhelum basin for 12 years (2013–2014) and 5 years (2015–2019), respectively. The model performance was evaluated by the values obtained for statistical coefficients, R^2 , NSE, KGE, PB, MAE, and RMSE for both the calibration and validation periods. During calibration period R^2 ranged from 0.783 to 0.808, NSE from 0.753 to 0.793, and PB from 2.7 to 5.1% and during validation period R^2 ranged from 0.80 to 0.83, NSE from 0.70 to 0.80, and PB from 2 to 6.8%. The results are acceptable with reasonable accuracy, indicating good model performance and a reliable association between hydrometeorological inputs and streamflow. Thus, the HEC–HMS model can be used for further studies related to climate change impact studies as a future scope of this study. The performance of the HEC–HMS model may further be enhanced by using the directly measured watershed parameters like soil texture, saturated hydraulic conductivity, soil tension storage, and infiltration rate of the soil.

Acknowledgements The authors are highly thankful for the assistance provided by the institute authorities and department of Civil engineering for providing the immense support to carry out this research. The authors are grateful to the Ministry of Human Resource Development (MHRD), Government of India, for providing funding support to carry out this research work.

Availability of data and materials Daily Meteorological data were obtained from Indian Meteorological Center (IMC) Rambagh, Jammu and Kashmir, India and measured data of Stages and corresponding discharge for the gauging stations were obtained from the department of irrigation and flood control, Jammu and Kashmir, India.

Declarations

Conflict of interest The authors declare that they have no conflict of interest.

References

- Alkaeed O, Flores C, Jinno K, Tsutsumi A (2006) Comparison of several reference evapo-transpiration methods for Itoshima peninsula area, Fukuoka, Japan. *Mem Fac Eng Kyushu Univ* 66(1):1–15
- Al-Mukhtar M, Al-Yaseen F (2019) Modeling water quality parameters using data-driven models, a case study Abu-Ziriq marsh in south of Iraq. *Hydrology* 6(1):24. <https://doi.org/10.3390/hydrology6010021>
- Altaf S, Romshoo SA (2022) Flood vulnerability assessment of the Upper Jhelum Basin using HEC-HMS model. *Geocarto Int* 1–20
- Arnold JG, Srinivasan R, Muttiah RS, Williams JR (1998) Large area hydrologic modelling and assessment. Part I: model development. *J Am Water Resour Assoc* 34:73–89. <https://doi.org/10.1111/j.1752-1688.1998.tb05961.x>
- Azizi S, Ilderomi AR, Noori H (2021) Investigating the effects of land use change on flood hydrograph using HEC-HMS hydrologic model (case study: Ekbatan Dam). *Nat Hazards* 109(1):145–160. <https://doi.org/10.1007/s11069-021-04830-6>
- Bashir T, Kumar R (2017) Simulation of modelling of water ecohydrologic dynamics in a multilayer root zone under protected conditions in the temperate region of India. *J Hydrol Eng* 22(10):05017020
- Bashir T, Romshoo SH, Sabha I (2018) Monitoring land use/cover change using remote sensing and GIS techniques in upper Jhelum basin. *Int J Adv Res Sci Eng* 7(4):1060–1077
- Baumbach T, Burckhard SR, Kant JM (2015) Watershed modeling using arc hydro tools. *Geo HMS, and HEC-HMS. Civ Environ Eng Fac Publ* 1–35
- Belayneh A, Sintayehu G, Gedam K, Gedam K, Muluken T (2020) Evaluation of satellite precipitation products using HEC-HMS model. *Model Earth Syst Environ* 6:2015–2032. <https://doi.org/10.1007/s40808-020-00792-z>
- Ben Khélifa W, Mosbahi M (2022) Modeling of rainfall-runoff process using HEC-HMS model for an urban ungauged watershed in Tunisia. *Model Earth Syst Environ* 8:1749–1758. <https://doi.org/10.1007/s40808-021-01177-6>
- Bennett T, Peters JC (2000) Continuous Soil Moisture Accounting in the Hydrologic Engineering Center Hydrologic Modeling System (HEC-HMS). In: *Proceedings of the 2000 Joint Conference on Water Resources Engineering and the Water Resources Planning and Management, Hyatt Regency Minneapolis, ASCE*
- Beven KJ (2011) *Rainfall-runoff modelling: the primer*. Wiley, Hoboken. <https://doi.org/10.1002/9781119951001>
- Bhuiyan HA, McNairn H, Powers J, Merzouki A (2017) Application of HEC-HMS in a cold region watershed and use of RADAR-SAT-2 soil moisture in initializing the model. *Hydrology* 4(1):9
- Biondi D, Freni G, Iacobellis V, Mascaro G, Montanari A (2012) Validation of hydrological models: conceptual basis, methodological approaches and a proposal for a code of practice. *Phys Chem Earth* 42:70–76
- Dimri T, Ahmad S, Sharif M (2022) Hydrological modelling of Bhagirathi River basin using HEC-HMS. *J App Water Eng Res* 1–13
- Fanta SS, Sime CH (2022) Performance assessment of SWAT and HEC-HMS model for runoff simulation of Toba watershed. *Ethiopia Sustain Water Resour Manag* 8(1):1–16
- Fleming M, Neary V (2004) Continuous hydrologic modeling study with the hydrologic modeling system. *ASCE J Hydrol Eng* 9:175–183
- Fontaine TA, Cruickshank TS, Arnold JS, Hotchkiss RH (2002) Development of a snowfall–snowmelt routine for mountainous terrain for the soil water assessment tool (SWAT). *J Hydrol* 262:209–223. [https://doi.org/10.1016/S0022-1694\(02\)00029-X](https://doi.org/10.1016/S0022-1694(02)00029-X)
- Gebre SL, Ludwig F (2015) Hydrological response to climate change of the upper Blue Nile River Basin: based on IPCC Fifth Assessment Report (AR5). *J Climatol Weath Forecast* 3:121
- Ghorbani K, Wayayok A, Abdullah AF (2016) Simulation of flood risk area in Kelantan watershed, Malaysia using numerical model. *J Teknol* 78(1–2):51–57
- Golmohammadi G, Prasher S, Madani A, Rudra R (2014) Evaluating three hydrological distributed watershed models: MIKE-SHE, APEX. *SWAT Hydrol* 1(1):20–39. <https://doi.org/10.3390/hydrology1010020>
- Graham DN, Butts MB (2005) Flexible, integrated watershed modeling with MIKE SHE. In: Singh VP, Frevert DK (eds) *Watershed models*. CRC Press, pp 245–272

- Gupta HV, Sorooshian S, Yapo PO (1999) Status of automatic calibration for hydrologic models: comparison with multilevel expert calibration. *J Hydrol Eng* 4:135–143
- Halwatura D, Najim MMM (2013) Application of the HEC-HMS model for runoff simulation in a tropical catchment. *Environ Modell Softw* 46:155–162. <https://doi.org/10.1016/j.envsoft.2013.03.006>
- Hamman JJ, Nijssen B, Bohn TJ et al (2018) The Variable Infiltration Capacity model version 5 (VIC-5): infrastructure improvements for new applications and reproducibility. *Geosci Model Dev* 11:3481–3496. <https://doi.org/10.5194/gmd-11-3481>
- Herath MH, Wijesekera NT (2021) Evaluation of HEC-HMS model for water resources management in Maha Oya Basin in Sri Lanka. *ENG* 54(02):45–53
- Ismael O, Sang Joseph K, Home Patrick G (2017) HEC-HMS model for runoff simulation in Ruiru reservoir watershed. *Am J Eng Res* 6(4):1–7
- Kabiri R (2014) Simulation of runoff using modified SCS-CN method using GIS system, case study: Klang watershed in Malaysia. *Res J Environ Sci* 8(4):178
- Kabiri R, Chan A, Bai R (2013) Comparison of SCS and Green-Ampt methods in surface runoff-flooding simulation for Klang Watershed in Malaysia. *Open J Modern Hydrol* 03(03):102–114. <https://doi.org/10.4236/ojmh.2013.33014>
- Kasa I, Gelybó G, Horel Á et al (2017) Evaluation of three semi-distributed hydrological models in simulating discharge from a small forest and arable dominated catchment. *Biologia* 72:1002–1009. <https://doi.org/10.1515/biolog-2017-0108>
- Kastali A, Zeroual A, Zeroual S, Hamitouche Y (2022) Auto-calibration of HEC-HMS model for historic flood event under rating curve uncertainty. Case Study: Allala Watershed, Algeria. *KSCE J Civil Eng* 26(1):482–93
- Kumarasamy K, Belmont P (2018) Calibration parameter selection and watershed hydrology model evaluation in time and frequency domains. *Water* 10(6):710. <https://doi.org/10.3390/w10060710>
- Leavesley GH, Lichty RW, Troutman BM, Saindon LG (1983) Precipitation runoff modeling system user's manual, water resources investigations 834238, Denver CO, Geological Survey: United States Department of the Interior
- Li Z (2014) Watershed modeling using arc hydro based on DEMs: a case study in Jackpine watershed. *Environ Syst Res* 3:11. <https://doi.org/10.1186/2193-2697-3-11>
- Markstrom SL, Regan RS, Hay LE, et al (2015) PRMS-IV, the precipitation-runoff modeling system, version 4, U.S. 25 1 Geological Survey Techniques and Methods, book 6, chap. B7, 158, 2. <https://doi.org/10.3133/tm6B7>
- Mobarhan EY, Sangchini EK (2021) Continuous rainfall–runoff modeling using HMS-SMA with emphasis on the different calibration scale. *J Chin Soil Water Conserv* 52(2):112–119
- Mohammed TA, Said S, Bardaie MZ, Basri SN (2011) Numerical simulation of flood levels for tropical rivers'. *IOP Conf Ser Mater Sci Eng* 7:1–10
- Ndeketea A, Dundu M (2021) Application of HEC-HMS model for evaluation of rainwater harvesting potential in a semi-arid city. *Water Res Manag* 35(12):4217–4232
- Othman N, Romali NS, Samat SR, Ahmad AM (2021) Calibration and validation of hydrological model using HEC-HMS for Kuantan River Basin. In: *IOP conference series: materials science and engineering* Mar 1 (Vol. 1092, No. 1, p. 012028). IOP Publishing
- Ouedraogo WAA, Raude JM, Gathenya JM (2018) Continuous modeling of the Mkurumudzi River catchment in Kenya using the HEC-HMS conceptual model: calibration, validation, model performance evaluation and sensitivity analysis. *Hydrology* 5:44
- Ramly S, Tahir W (2016) Application of HEC-GeoHMS and HECHMS as rainfall–runoff model for flood simulation. In: *ISFRAM 2015*. Springer, Singapore, pp 181–192. https://doi.org/10.1007/978-981-10-0500-8_15.
- Ranjan R, Dhote PR, Thakur PK, Aggarwal SP (2022) Investigation of basin characteristics: implications for sub-basin-level vulnerability to flood peak generation. *Nat Hazard* 6:1–33
- Razmkhah H, Saghafian B, Akhound Ali A, Radmanesh F (2016) Rainfall-runoff modeling considering soil moisture accounting algorithm, case study: Karoon III River basin. *Water Resour* 43(4):699–710
- Roy D, Begam S, Ghosh S, Jana S (2013) Calibration and validation of HEC–HMS model for a river basin in eastern India. *ARPN J Eng Appl Sci* 8:40–56
- Sahu S, Pyasi S, Galkate R (2020) A review on the HEC-HMS rainfall–runoff simulation model. *Int J Agric Sci Res* 10(4):183–190
- Scharffenberg W, Ely P, Daly S et al (2010) Hydrologic modeling system (HEC-HMS): physically-based simulation components. 2nd Joint Federal Interagency Conference, Las Vegas, NV
- Shah M, Lone MA (2021) Hydrological modeling to simulate stream flow in the Sindh Valley watershed, northwest Himalayas. *Model Earth Syst Environ* 2:2461–2470. <https://doi.org/10.1007/s40808-021-01241-1>
- Shakarneh MOA, Khan AJ, Mahmood Q (2022) Modeling of rainfall–runoff events using HEC-HMS model in southern catchments of Jerusalem Desert-Palestine. *Arab J Geosci* 15:127. <https://doi.org/10.1007/s12517-021-09406-z>
- Sime CH, Demissie TA, Tufa FG (2020) Surface runoff modeling in Ketar watershed, Ethiopia. *J Sediment Environ* 5:151–162. <https://doi.org/10.1007/s43217-020-00009-4>
- Singh WR, Jain MK (2015) Continuous hydrological modeling using soil moisture accounting algorithm in Vamsadhara river basin, India. *J Water Res Hydraul Eng* 4:398–408
- US Army Corps of Engineers (1998) HEC-1 flood hydrograph package user's manual. Hydrologic Engineering Center, Davis, CA, USA
- US Army Corps of Engineers (2000) HEC-HMS, Hydrologic Modeling System User's Manual, Hydrologic Engineering Center, Davis, CA, USA
- US Army Corps of Engineers (2013) Hydrologic Engineering Center, HEC. HEC-GeoHMS, Users' Manual
- US Army Corps of Engineers (2020) Hydrological Center (CEIWR-HEC) Hydrologic Modelling System (HEC-HMS) Hydrologic Engineering Center (CEIWR-HEC)

Publisher's Note Springer Nature remains neutral with regard to jurisdictional claims in published maps and institutional affiliations.

Springer Nature or its licensor holds exclusive rights to this article under a publishing agreement with the author(s) or other rightsholder(s); author self-archiving of the accepted manuscript version of this article is solely governed by the terms of such publishing agreement and applicable law.